Response modulation by texture surround in primate area V1: Correlates of "popout" under anesthesia

HANS-CHRISTOPH NOTHDURFT,[1,2] JACK L. GALLANT,[1,*] AND DAVID C. VAN ESSEN[1,**]

[1]Division of Biology, California Institute of Technology, Pasadena
[2]Max Planck Institute for Biophysical Chemistry, Department of Neurobiology, Goettingen, Germany

Abstract

We studied the effects of contextual modulation in area V1 of anesthetized macaque monkeys. In 146 cells, responses to a single line over the center of the receptive field were compared with those to full texture patterns in which the center line was surrounded by similar lines at either the same orientation (*uniform texture*) or the orthogonal orientation (*orientation contrast*). On average, the responses to single lines were reduced by 42% when texture was presented in the surround. Uniform textures often produced stronger suppression (7% more, on average) so that lines with orientation contrast on average evoked larger responses than lines in uniform texture fields. This difference is correlated with perceptual differences between such stimuli, suggesting that physiological mechanisms contributing to the saliency ("popout") of textural stimuli operate, at least to some degree, even under anesthesia. Significant response modulation by the texture surround was seen in 112 cells (77%). Fifty-three cells (36%) responded differently to the two texture patterns; response preferences for orientation contrast (35 cells; 24%) were seen more often than preferences for uniform textures (18 cells; 12%). The remaining 59 cells (40%) were similarly suppressed by both texture surrounds. Detailed analysis of texture modulation revealed two major components of surround effects: (1) fast nonspecific ("general") suppression that occurred at about the same latency as excitatory responses and was found in all layers of striate cortex; and (2) differential response modulation that began about 60–70 ms after stimulus onset (about 15–20 ms after the onset of the excitatory response) and was less homogeneously distributed over cortical layers.

Introduction

One problem in understanding the neural basis of visual perception is the link between the mosaic-like representation of visual information in the early visual system and the global perception of spatially extended objects. While filter properties of neurons at early stages of processing have been studied extensively, we know relatively little about the way they encode large-scale aspects of the visual world.

Several studies have reported that responses in V1 can be strongly modulated by stimuli outside the "classical" excitatory receptive field (RF). While earlier reports linked this interaction to specific subregions of the RF (inhibitory endzones or sidebands; Hubel & Wiesel, 1965, 1968; Henry & Bishop, 1971; Dreher, 1972; Bishop et al., 1973; Kato et al., 1978), later studies have demonstrated that such influences extend far beyond these local modulatory zones (e.g. Allman et al., 1990; Gilbert & Wiesel, 1992; Knierim & Van Essen, 1992; DeAngelis et al., 1994; Li & Li, 1994; Kapadia et al., 1995; Sillito et al., 1995; Zipser et al., 1996). The stimulation of silent regions outside the RF can modify a cell's sensitivity even in the absence of driving stimuli (Gilbert & Wiesel, 1992; Das & Gilbert, 1995), which illustrates their important role in perpetual cortical plasticity. These observations clearly indicate that cells in the primary visual cortex are not simply local filters whose processing is limited to the stimulus over the RF, but must be seen as part of a network that is modulated by stimulus context.

Although there is now general agreement on the existence of contextual modulation in V1, there seems to be some controversy about which stimuli evoke which effects. For example, stimuli oriented parallel to the cell's optimum and bars aligned with the driving stimulus over the RF have been found to produce strong suppression (Orban et al., 1979; DeAngelis et al., 1994; Li & Li,

Correspondence and reprint requests to: Hans-Christoph Nothdurft, Max Planck Institute for Biophysical Chemistry, D-37070 Goettingen, Germany.
*Present address: 3210 Tolman Hall #1650, U.C. Berkeley, Berkeley, CA 94720-1650, USA.
**Present address: Department of Anatomy and Neurobiology, Washington University School of Medicine, St. Louis, MO 63110, USA.

1994), but facilitatory effects have recently been reported as well (Kapadia et al., 1995). Several studies have demonstrated specific suppression from global stimulation of the RF surround (e.g. Blakemore & Tobin, 1972; Fries et al., 1977; Nelson & Frost, 1978; Allman et al., 1990; Born & Tootell, 1991; Knierim & Van Essen, 1992; Li & Li, 1994; Sillito et al., 1995; Kastner et al., 1997); other studies found primarily nonspecific inhibition (e.g. Maffei & Fiorentini, 1976) or reported other preferences (Gilbert & Wiesel, 1990). While many of these studies were done on anesthetized animals, mainly cats, some studies were performed on alert monkeys, and it is possible that the level of anesthesia or differences between these species might have affected the strength and specificity of modulatory effects obtained in different studies. This is also suggested from a recent report according to which contextual modulation is eliminated under anesthesia (Zipser et al., 1997). Other studies, however, have seen such modulation effects even in anesthetized preparations (e.g. Gilbert & Wiesel, 1990; DeAngelis et al., 1994; Li & Li, 1994; Sillito et al., 1995; Kastner et al., 1997).

Modulatory effects are not always linked absolutely to the structure of surround stimuli but can also depend on relative properties to the stimulus in the RF. Differences in orientation or direction or speed of motion between stimuli within and outside the RF (feature contrast) often produce increased responses irrespective of the orientation, or direction of the stimulus in RF (Hammond & Smith, 1982, 1984; Allman et al., 1985, 1990; Gulyas et al., 1987; Orban et al., 1987; Knierim & Van Essen, 1992; Lamme, 1995; Sillito et al., 1995; Zipser et al., 1996; Kastner et al., 1997); such responses are also seen in visually evoked potentials (Bach & Meigen, 1992, 1997; Lamme et al., 1992, 1993a,b, 1994). Knierim and Van Essen (1992) investigated contextual modulation in awake monkeys, using texture stimuli often used in psychophysics. About one-third of their sample of V1 cells responded more strongly to a line surrounded by orthogonal lines than to the same line surrounded by lines at the same orientation. Perceptually these stimuli are quite distinct. Lines surrounded by orthogonal lines are more salient than lines embedded in similar lines; they "pop out" (Beck, 1967; Treisman & Gormican, 1988; Foster & Ward, 1991; Nothdurft, 1991, 1992).

Popout is obtained from a variety of stimulus properties including differences in depth, motion, color, or orientation (Julesz, 1971, 1975; Treisman, 1985; Nakayama & Silverman, 1986; Nothdurft, 1993a, 1995). Because many of these properties are represented explicitly by neurons in the primary visual cortex, it was originally thought that popout may reflect the activation of specific cells in this area, thus signaling the presence of specific features associated with the popout target. But then it was found that the same target may or may not pop out depending on stimulus context (Duncan & Humphreys, 1989; Moraglia, 1989; Nothdurft, 1991, 1992), and perceptual popout was instead related to orientation differences and local feature contrast (Nothdurft, 1991, 1993a,b, 1995). If a line embedded in dissimilar lines (the "popout" condition) produces stronger responses in area V1 than a line surrounded by similar lines, then target salience and hence popout might be encoded in the general strength of responses rather than in the specific responses of labeled feature detectors (cf. Nothdurft, 1994a). Similar effects may help to detect texture boundaries, a perceptual phenomenon probably closely related to popout (Beck, 1982; Nothdurft, 1991, 1994b, 1997; Sagi, 1995).

Motivated by these issues, we carried out two sets of tests on cells in area V1 of anesthetized macaque monkeys. In the present study, we report on the responses of cells to single lines in the RF that were surrounded by lines having the same or the orthogonal orientation (the "uniform texture field" *vs.* the "popout" condition). Here, we compare these data to those obtained in a similar study in the alert monkey (Knierim & Van Essen, 1992). The present study also provides a useful baseline for comparisons with responses of the same population of cells to texture borders, which will be reported in a separate paper (Nothdurft, Gallant, & Van Essen, submitted).

Methods

Recordings were made from four anesthetized, paralyzed macaque monkeys (*Macaca nemestrina*) in acute experimental procedures. Appropriate doses for anesthesia were determined for each animal before paralysis and, if necessary, continuously adjusted during the experiment. All procedures were carried out under institutionally approved protocols and conformed to the NIH Guidelines for the Care and Use of Animals.

Preparation

Methods for surgery and acute recording were similar to those previously described (Felleman & Van Essen, 1987; Olavarria et al., 1992; Gallant et al., 1996). All surgery was done under general anesthesia (2.5–4.5% isoflurane in air containing 2.5% CO_2) and under aseptic conditions. A stainless-steel cylinder was mounted on the skull and fixed by means of bone screws and dental cement. During recording the cylinder was filled with sterile mineral oil and sealed. Electrodes were inserted approximately normal to the pial surface through a sealed opening in the recording chamber and were advanced into the brain through small holes in the skull (typically 3–4 mm diameter) that were drilled within the aperture of the cylinder.

In one animal the chamber was implanted in a separate survival surgery prior to the physiological recording experiment. Buprenex (0.01–0.03 mg/kg) and tylenol were administered to minimize postsurgical discomfort. With this animal, the acute surgery immediately before the experiment was limited to craniotomy. In all other animals, full surgery was performed immediately before the recording session.

After surgery, animals were switched from isoflurane to a continuous infusion of sufentanil citrate (5–8 μg/kg/h, i.v.); an initial bolus of sufentanil was given before continuous infusion. Anesthesia was adjusted for each animal throughout the experiment by monitoring EKG rate (90–150 beats/min) and EEG state (predominance of low-wave activity), and by periodically testing for absence of EKG or EEG responses to toe pinch. Once proper anesthesia was obtained, paralysis was induced with gallamine triethiodide (10 mg/kg/h, i.v.). Animals were respirated through a tracheal cannula with a mixture containing 2.5% CO_2 in air, or with air alone.

After paralysis atropine (2%) and neo-synephrine were placed into the eyes which then were covered with neutral contact lenses and artificial pupils (4 mm diameter). Corrective lenses were used to focus the eyes on a tangent screen 114 cm away from the animal. Foveal positions were plotted using a reversing-beam ophthalmoscope, and the foveae of both eyes were aligned on the screen by means of prisms in front of one or both eyes. For recordings, however, stimuli were always presented to only one eye, whichever was most effective for each cell; the other eye was occluded. Eye condition and alignment were checked periodically throughout the experiment.

Experiments lasted up to 5 days during which time the animals received regular massages to ensure good blood circulation, and periodic injections of amino acids (Vet Labs Oral Solution, 3 ml/ 4 h, i.v.) and vitamin B complex (0.75 ml/day). Body temperature was maintained at 37–38°C with a water heating pad.

Recording and RF analysis

Extracellular single-unit recordings were made with Levick-style microelectrodes (tungsten-in-glass) inserted into para-foveal striate cortex. We tried to record from as many neurons as possible in long penetrations that often reached down into the calcarine fold.

After isolating a single unit, receptive-field properties were investigated using stationary and moving bars of various colors. Initial RF estimates were made using a customized plotting program which allowed for mouse-controlled movement of stimuli and interactive variation of stimulus properties. RF size was defined as the minimal response field (Barlow et al., 1967), and the optimal bar size and orientation were determined by hand. No attempt was made to classify cells as simple, complex, or hypercomplex, although such a distinction was evident for some cells. Various colors were tested, including dark bars on a bright background, but the spectral sensitivity of the cells was not studied in detail. The major goal was simply to find an effective stimulus that evoked a strong response when presented in the RF. Properties such as sensitivity to motion, orientation selectivity, and ocular dominance, as well as general aspects of recording quality, briskness of response, and spike amplitude were also recorded. These records allowed us to estimate the layers cells were drawn from (e.g. cells in layer 4C typically had a brisk firing rate, low orientation selectivity, and small spike amplitude). Once the RF was plotted by hand and an optimal stimulus was found, a series of computer-controlled tests were run to center the stimulus within the RF. In these tests, stimulus position was systematically varied in steps of 0.05–0.1 deg and response profiles were obtained for the two main axes of the RF. Stimulus locations that evoked the maximal response were then taken as the center line position for texture fields.

Texture stimuli

As illustrated in the sketches of Fig. 1, stimuli consisted of a central bar (C or C′) and a pattern of identical lines in the surround (S or S′). Surround stimuli extended all over the screen and displayed many more lines than sketched in Fig. 1. Lines were either parallel (C, S) or orthogonal (C′, S′) to the cell's preferred orientation. Combinations of center bars and surrounds produced two global test conditions: *uniform textures* (C/S, C′/S′) with all lines at the same orientation, and *popout patterns* (C/S′, C′/S) with orientation contrast between the center line and the surround that made the center line "pop out." Responses to these patterns were compared with the responses to centers or surrounds alone. In all but one animal modulatory effects were measured for both optimal (C) and nonoptimal (C′) center lines, and tests included all the stimulus conditions depicted in Fig. 1. In the first experiment, only textures with an optimally oriented center (C, C/S, C/S′) were tested and no controls were run to examine responses to surrounding textures alone.

Texture stimuli were constructed from the bars that evoked the strongest response in the RF (see above) and thus were optimized in texel size, color, and orientation for each individual cell. The resulting patterns for different cells were rotated and scaled ver-

sions of one another, but could differ in texel width and color. Texture patterns were constructed according to the following rules: (1) The length and width of surround texture elements ("tex-els") were identical to the center line, which itself was optimized for each cell as described above. (2) Texels were arranged in a rectangular grid with axes oblique (±45 deg) to texel orientation. (3) Texel spacing (along these oblique axes) was 1.5 times the length of the texels. With this spacing, texels in the surround were usually well outside the excitatory RF. On the rare occasions when surrounds with this standard spacing evoked a response from the cell, the texel spacing was increased up to two times the texel length. In some cells smaller and larger spacings were also tested. (4) To avoid that popout effects are confounded by local luminance inhomogeneities in the pattern (Nothdurft, 1990), irregular texture grids were generally used. Except for the center line over the RF, a small positional jitter (up to 30% of texel spacing) was applied to each texel; this jitter was randomly assigned for every new stimulus presentation. Texture patterns with this geometry have also been used in psychophysical experiments (Nothdurft, 1985*a*, 1992). We used texels of 0.23–1.77 deg length and 0.02–0.24 deg width; mean values were 0.61 deg × 0.091 deg. Width/length ratios varied from 4.6% to 37%, with a mean of 15%.

Stimuli were presented on a 19-inch RGB raster monitor (1280 by 1024 pixels; 66-Hz frame rate noninterlaced) giving an effective size of 18.5 by 14.8 deg of the visual field. Texture patterns covered the entire screen and contained many more elements than shown in the schematic drawings of Figs. 1–3. While there was only one center element, the number of texels in the surround depended on texel length and texel spacing. For a mean texel length of 0.6 deg and the usual 1.5-fold texel spacing, texture surrounds contained more than 300 texels. Luminance variations associated with different line orientations were small and did not produce perceptible differences in mean luminance when the screen was blurred. Texture patterns were shown in one of eight colors (white, dark blue, green, light blue, red, magenta, yellow, or black), selected so as to produce a good response to a single line over the RF. All tests with a particular cell were made using the same color on a neutral background. Because colors were not equated for luminance, the effective texel luminance contrast differed between cells.

Data acquisition and analysis

Spikes were collected and stored on a Macintosh IIfx that also controlled test sequences and stimulus parameters. Stimulus specifications were transferred to a separate computer (Masscomp Aurora Graphics, La Jolla, CA) where the actual texture patterns were generated and timing of the display was controlled. Both systems were synchronized by brief small flashes on the graphics monitor (hidden from the animal) that were detected by a photodiode. Detailed analysis of response properties was done off-line.
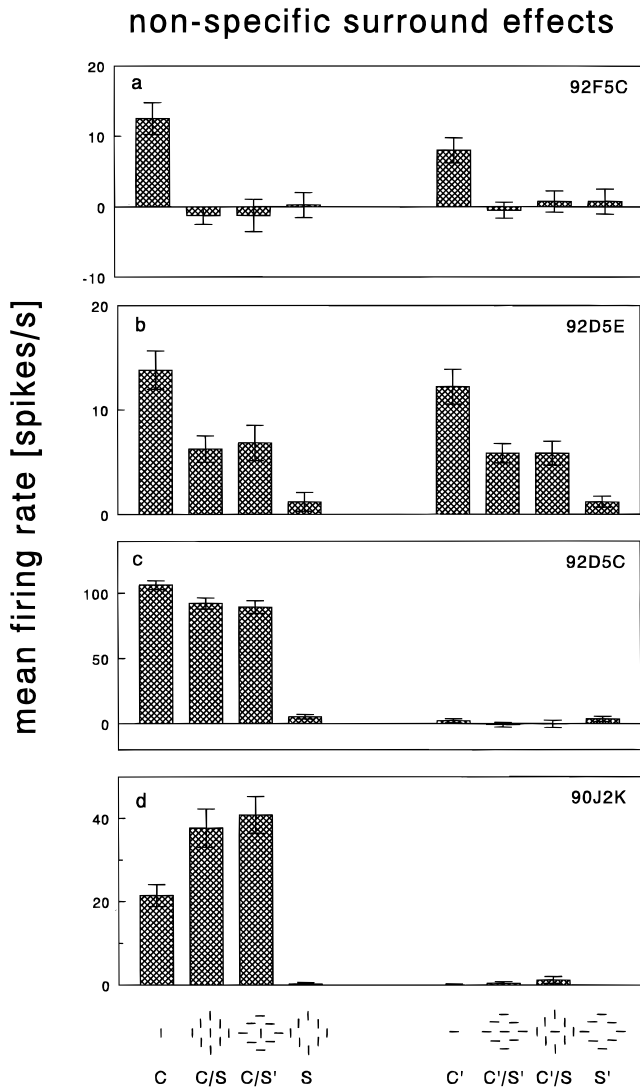
On each trial, spontaneous activity was measured during the 500-ms epoch before stimulus presentation. Stimulus patterns were then shown for 500 ms, but recording continued for another 250–500 ms depending on the strength of a cell's off response. Cells that responded to both the onset and the offset of stimuli generally showed similar variation with texture conditions in their on and off responses. However, in this report we have not analyzed off responses except for four cells that showed no response to the onset of the center line. The intertrial interval was 1–3 s. Different test conditions were shown in pseudorandom order, and all conditions of a particular test series were shown before repetition.
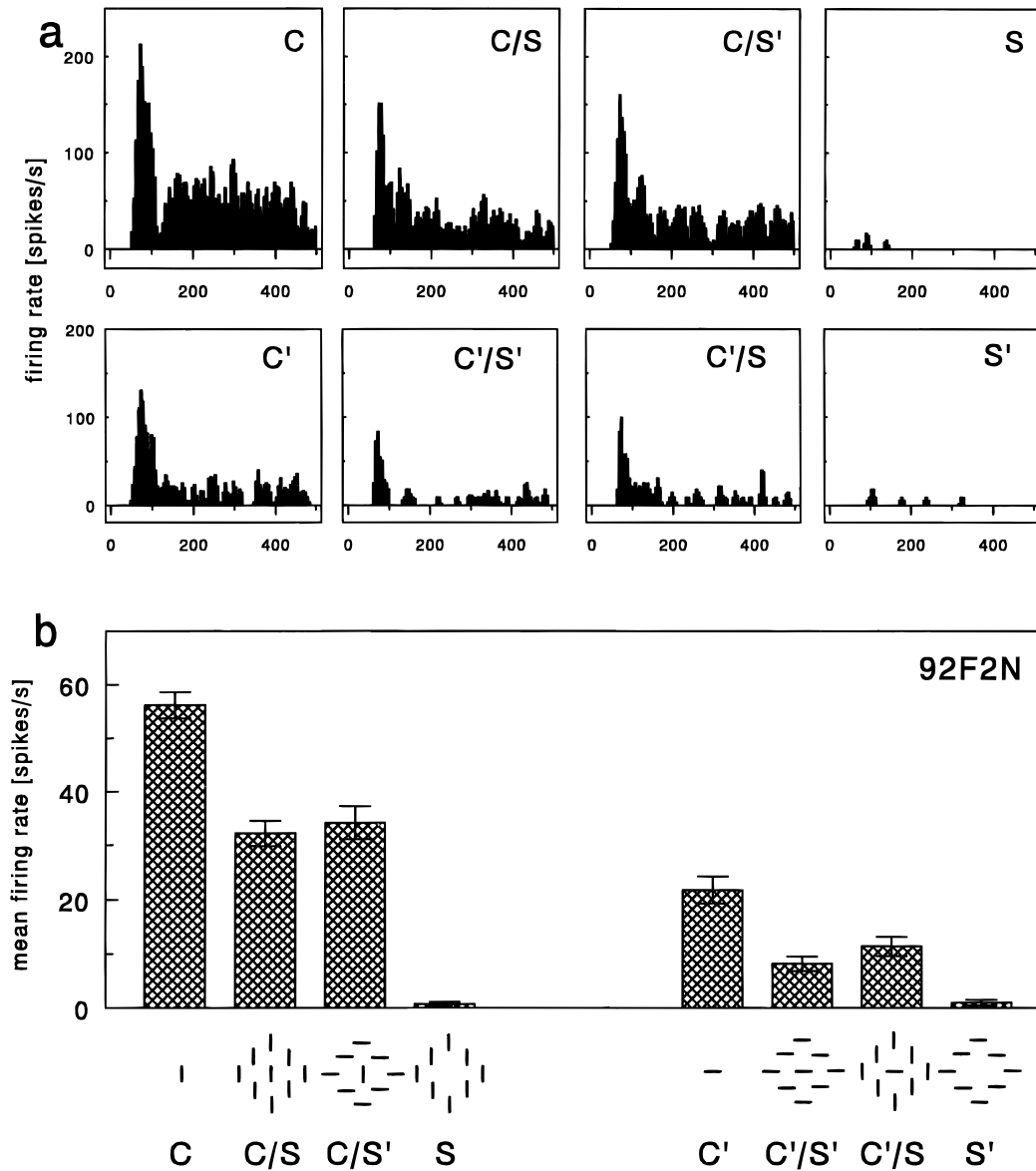
Fig. 1. Responses of a V1 cell to the different texture conditions tested. An optimal bar over the "classical" receptive field (RF) was presented alone or together with a texture surround located outside the RF. Combinations of center lines and texture surrounds produced uniform textures (all lines at the same orientation) or textures with orientation contrast (surrounding lines orthogonal to the center line). Line elements were individually adjusted to a cell's RF and usually patterns with optimal and orthogonal center lines (prime symbols) were tested. Texture stimuli covered the whole monitor. (a) Response histograms to textures with optimal (upper row) and orthogonal center lines (lower row) in the RF; 10 repetitions. (b) Mean responses over the full presentation time (500 ms) as computed from histograms in (a); error bars give standard errors of the mean. The responses to the optimal center line (condition C) were suppressed by either texture surround (conditions C/S and C/S′) as were the responses to the orthogonal center line (conditions C′, C′/S′, and C′/S). Texture surrounds alone (conditions S and S′) did not evoke a response. Mean response histograms as in (b) will be used for the description of response properties in the following pictures. Stimulus configurations in this and subsequent figures are schematic; vertical bars always represent the optimal orientation of the cell.

Spikes were stored with 1-kHz resolution. While temporal response properties were analyzed using peri-stimulus time histograms at this resolution, most analyses in this paper are based on mean responses of a cell averaged over the full period of stimulus presentation. Responses from individual trials were averaged over all repetitions of each stimulus condition (usually 10–20) and standard errors of the mean (S.E.M.) were used to estimate the reliability of a given response difference in a single cell (see below).

Spontaneous firing rates were always subtracted from the means before analysis so that the values given in this paper represent the cell's evoked response rate to the texture stimuli. For cells with high spontaneous activity, response rates can thus be negative if texture patterns suppressed activity. Most analyses used estimates of *mean* firing rates; hence, cells with a strong transient response may appear less responsive than cells with a weaker sustained response.

non-specific surround effects

preference for orientation contrast

preference for uniform texture

Fig. 2. Response patterns of cells which showed nonspecific modulatory effects from texture surrounds. Test conditions are as in Fig. 1. Examples were selected to illustrate the variation of texture modulation observed in the experiments. (a–c) Generally suppressed cells as that in Fig. 1; the responses to the center line (condition C) were similarly suppressed by both texture surrounds (conditions C/S and C/S′), although the strength of suppression varied between cells. (d) General enhancement by texture surround; responses to the center line were enhanced by either texture surround. Surrounds alone evoked only minor responses (S, S′). General suppression was far more frequent than general enhancement. It was also seen with orthogonal center lines (right half of each graph) if cells responded to those.

Response properties were quantified in terms of several indices defined below. When distributions of some of these indices over the population were analyzed in detail, significance estimates were generally based on one-sample (student's) *t*-tests and paired or independent *t*-test analysis. To test for statistical significance of latency differences across cell groups, we applied two methods to estimate response latencies of individual cells. Row histograms (1-ms resolution) were first smoothed using a shifting rectangular time window of 23 ms. In method 1, values were then checked if they exceed spontaneous firing rate by a threshold set to 10% of the cell's peak response for this test (spontaneous firing rate sub-
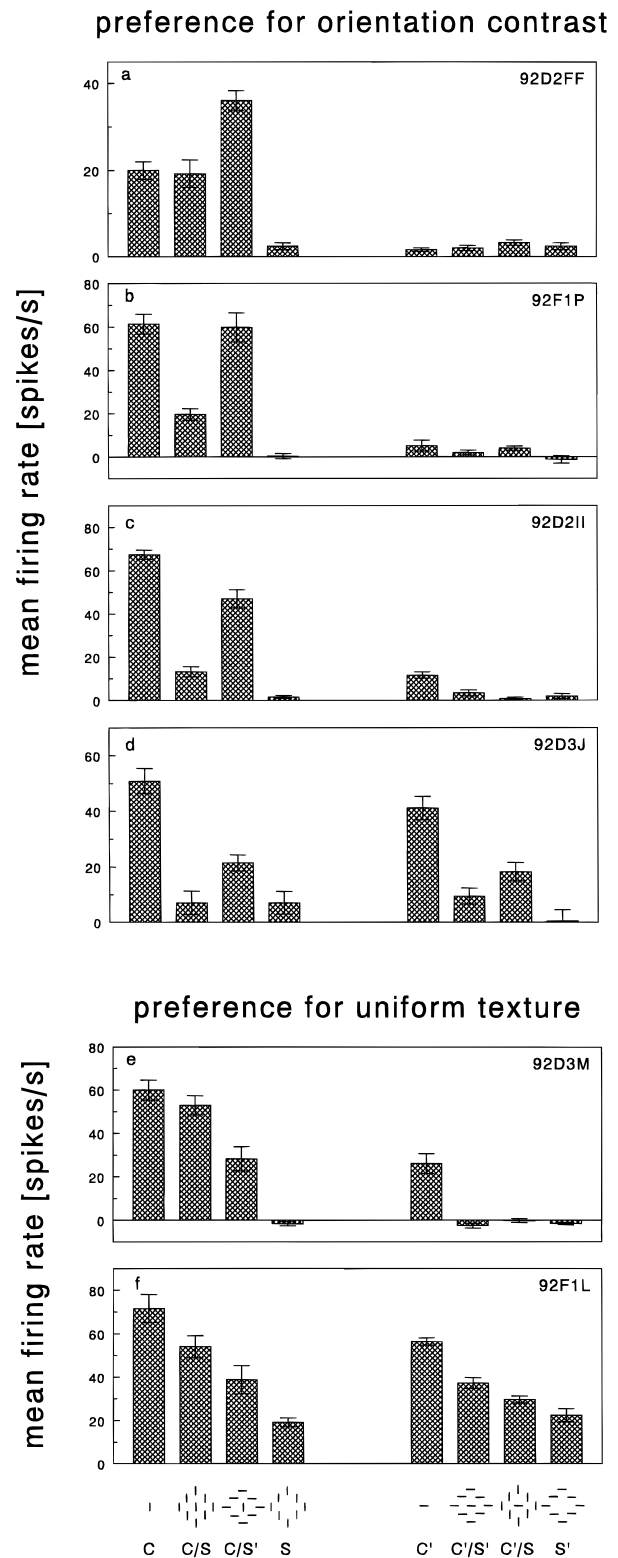
Fig. 3. Response patterns of cells with specific modulatory effects. (a–d) Preferences for orientation contrast (C/S < C/S′) were seen more frequently than (e,f) preferences for uniform textures (C/S > C/S′). Response differences could be based on selective enhancement (a) or differential suppression (b–f). Even surrounds that evoked a response from the cell when presented alone could produce differential suppression when presented in combination with the center line (d,f). Test conditions are as in Figure 1.

tracted). If this occurred for 20 values in sequence, the time of the first value (plus half of the smoothing window) was taken as the first measure of response latency. In method 2, response differences were computed along the smoothed histogram, between data points 6 ms before and 6 ms after the actual position. If ten such differences in sequence were found to be positive, the time of the first one (plus 12 ms plus half of the smoothing window) was taken as the second measure of response latency. Finally, both these values were averaged to give the response latency of a cell to one particular stimulus condition. Although this measure was defined *ad hoc*, it gave similar results as occasional direct estimates from the histograms by hand.

Results

Our analysis is based on the responses obtained from 146 cells in area V1 with receptive fields within 15 deg from the fovea, which were selected for giving clear responses to the onset or offset of a single bar in the RF and no or minor responses to the texture surround presented alone. Seven units were judged to be fibers from the lateral geniculate nucleus (LGN) and were excluded from the analysis presented here. Although we tried to study as many neurons as possible in every penetration, not all cells could be stimulated well enough with flashed patterns, or were held long enough for full texture analysis. Brief recordings were made from over 200 cells. About 10% of these (22 out of 210 tested for response differences with moving and stationary stimuli) gave vigorous responses to a moving bar but failed to respond when the stimulus was flashed over the RF; these cells were not studied further.

Overview of responses to texture fields

Nonspecific surround effects

Fig. 1 illustrates the analysis of response properties performed on each cell. The cell depicted here gave a brisk sustained response to a white bar over the RF, with moderate orientation selectivity (C, bar at optimal orientation; C′, orthogonal bar). These responses were strongly reduced when a surrounding texture field was added, independent of the orientation of texels in the surround. Texture surrounds alone did not evoke a response from the cell (S, lines at the cell's preferred orientation; S′, lines orthogonal).

The histograms in Fig. 1b represent the mean responses (mean firing rate during stimulus presentation minus spontaneous firing rate) obtained in different stimulus conditions. Error bars give the standard error of the mean (S.E.M.) computed from individual trials; this measure reflects the response variability between repeated presentations of the same stimulus condition.

General suppression of center line responses by either texture surround as seen with this neuron was frequently observed in V1 cells. The strength of suppression varied considerably from cell to cell, as illustrated in Figs. 2a–2c; strong and even complete suppression was seen as well as medium or mild effects. The opposite effect, a general enhancement of center line responses by texture surrounds, was observed in only two cells (Fig. 2d).

Differential surround effects

In many cells, the two texture surrounds had different modulatory effects (Fig. 3). In most cases, texture fields with orientation contrast (the "popout" condition) produced stronger responses than uniform texture fields, but reversed preferences were also seen.

These differences were brought about by different mechanisms: reponse enhancement by the surround with orthogonal texels (Fig. 3a), selective suppression by texels at the same (optimal) orientation as the center line (Fig. 3b), and differential suppression from both surrounds (Figs. 3c and 3d). Cells with a preference for uniform texture were found less frequently than cells preferring orientation contrast, and tended to be less selective for orientation (Figs. 3e and 3f).

Nonlinearity of surround effects

The interactions between center bars and texture surrounds could be highly nonlinear, as illustrated in Figs. 3d and 3f. These cells showed mild responses to the surrounds presented alone (although we tried to adjust texel spacing so that these responses were minimized). Responses to full texture patterns, however, were not the linear sum of center and surround responses. For example, the cell in Fig. 3d responded weakly to the surround with texels at the optimal orientation (condition S) but not to the surround with orthogonal lines (condition S′). When texture surrounds were presented together with different center lines, the cell always preferred the orientation contrast condition, even when texels in the surround were orthogonal to the cell's optimum (condition C/S′). For the cell in Fig. 3f, both texture surrounds evoked a response when presented alone. Although these responses were similar in strength, the cell showed a clear preference for uniform texture patterns with either center line. Thus, even texture surrounds that activate a cell when presented alone may produce suppression (possibly differential) when shown together with the center lines.

Responses to textures with nonoptimal center lines

While some cells were orientation selective and responded only to an optimally oriented center line (e.g. Figs. 2c and 2d), quite a few cells were also activated by orthogonal center lines, thus allowing the modulatory effects of different center lines to be compared. As Figs. 3d and 3f show, differential effects were not necessarily linked to texel orientation in the surround but cells could maintain their preferences (for either popout or uniform texture type) for different orientations of the center line. Other cells showed different effects for different center lines (e.g. Fig. 3e).

Response categories

Based on this qualitative description of response properties in V1, we classified cells into three categories:

1. *Orientation contrast (OC)* cells whose mean responses to texture contrast exceeded responses to uniform textures by more than two S.E.M. ($R_{C/S'} - \text{S.E.M.} > R_{C/S} + \text{S.E.M.}$; with R_x denoting the cell's response to stimulus condition x and S.E.M. denoting the according standard error of the mean).

2. *Uniform (UF)* cells whose responses to uniform texture exceeded those to contrasting textures by more than two S.E.M. ($R_{C/S} - \text{S.E.M.} > R_{C/S'} + \text{S.E.M.}$).

3. *Generally suppressed (GS)* cells whose responses to the center lines were greatly suppressed by both texture surrounds ($R_C - \text{S.E.M.} > R_{C/S} + \text{S.E.M.}$; $R_C - \text{S.E.M.} > R_{C/S'} + \text{S.E.M.}$) and failed to show one of the above preferences for orientation contrast or uniform texture.

All other cells were classified as to show no effect ("n.e.").

No separate category was established for the few generally enhanced cells (two out of 146, cf. Fig. 2d) which were included in the n.e. group. Note that although each cell was assigned to a single group, cells could display characteristics of more than one category. For example many differential cells (OC and UF classes) also displayed a considerable amount of general suppression (cf. Figs. 3c–3f).

Our classification scheme was related to that of Knierim and Van Essen (1992) but differed in several aspects. In particular, our categories were based on responses for one center line orientation alone; hence different classifications were obtained for optimal and orthogonal center lines.

When tested with optimal center lines, most cells fell into the GS category (59/146 = 40%) but a similar proportion of cells showed differential responses to the two texture conditions (53/146 = 36%). Among these, OC cells (35/146 = 24%) were about twice as frequent as UF cells (18/146 = 12%) which made up only one-eighth of the sample. Only 23% (34/146) of the cells showed no effects according to our criteria. This distribution was similar for orthogonal center lines, but categories could differ in the cells.

Differences across center lines

We compared response categories for 90 cells that were tested with both optimal and orthogonal center lines and responded to the nonoptimal orientation with at least 10% of the optimum response (Table 1). The scatter of response categories for different center lines is only partly due to noise from the smaller responses to nonoptimal stimuli. In fact, the scatter was similar when analysis was restricted to cells that responded well (mean responses >10 spikes/s) to both center lines ($N = 65$). Interestingly, the different categories obtained with optimal center lines were not scattered in the same way for orthogonal centers. Most GS cells (as classified with the optimal center lines) were also GS for orthogonal centers (30/43 = 70%), whereas only 24% (8/33) of the cells with differential responses (OC cells, UF cells) retained their preferences (for either orientation contrast or uniform texture) for the orthogonal center line orientation. Most of them actually lost their differential response properties and became GS or n.e. type (cf. Fig. 3e). Only six cells (6/90 = 7%) showed opposite response preferences (the OC/UF and UF/OC classes in Table 1), suggesting that the interaction in these cells was related to the texel orientation in the surround.

Because the smaller responses to nonoptimal center lines presumably contributed little to the overall response properties of the population, we repeated the classification using a measure of *generalized* response properties (Table 2). Responses to textures surrounding different center lines were weighed by the strength of a cell's response to each center line alone, and averaged over similar texture conditions (uniform *vs.* contrast):

$$\langle R \text{ (uniform)} \rangle = (R_{C/S} \cdot R_C + R_{C'/S'} \cdot R_{C'})/(R_C + R_{C'}),$$

$$\langle R \text{ (contrast)} \rangle = (R_{C/S'} \cdot R_C + R_{C'/S} \cdot R_{C'})/(R_C + R_{C'}).$$

There were only small deviations between response categories determined by responses to optimal center lines and those given by the generalized responses; 86% of the cells (77/90) fell in the same category in each classification. For the remaining 13 cells (14%), generalized responses were always less specific (GS, n.e.) than those obtained with optimal center lines. This analysis suggests that response properties are well described by response categories based on stimuli with optimal center lines.

Table 1. *Response categories for optimal (rows) and nonoptimal center lines (columns) for cells whose responses to orthogonal center lines were at least 10% of those to optimal centers*

	GS	OC	UF	n.e.	Sum
GS	30	5	3	5	43
OC	5	6	2	7	20
UF	5	4	2	2	13
n.e.	1	5	0	8	14
Sum	41	20	7	22	90

Comparison with the scheme of Knierim and Van Essen (1992)

Knierim and Van Essen (1992) used a combination of optimal and orthogonal center line responses to classify cells. Based on response differences between these conditions, they also defined additional classes such as "center-dependent" or "surround-dependent suppression." We did not apply their scheme in the present study, because some of our cells were tested with only one center line orientation and because we found the classification based on one center orientation easier to apply and easier to interpret. However, in order to relate our data to theirs, we reclassified all 122 cells of our sample that were tested with two center line orientations, according to their scheme. Our sample then contained 41% GS cells (50/122), 26% OC cells (32/122), 11% UF cells (13/122), and 19% cells with no effect (23/122). Only 2% of the cells showed "surround dependent suppression" (3/122) and only 1% "center dependent suppression" (1/122). These data are similar although not identical to those for the alert monkey (Knierim & Van Essen, 1992; see Discussion).

Population means

While the responses of OC cells are consistent with the particular saliency of popout targets seen in psychophysical studies (Treisman & Gormican, 1988; Foster & Ward, 1991; Nothdurft, 1991, 1992), the responses of UF cells seem to be contrary to that effect. We therefore wished to know whether response differences of OC cells and UF cells cancel each other in the mean response of the population, or whether one or the other response preference might predominate.

Fig. 4A shows the mean responses to the various texture conditions of all 35 OC cells in the sample. The preference for orientation contrast over uniform texture fields was pronounced in these cells (paired *t*-test; $t = 10.5$, $P < 10^{-11}$). Although the mean

Table 2. *Response categories for optimal center lines (rows) and weighted means (columns) for the same sample as in Table 1*

	GS	OC	UF	n.e.	Sum
GS	40	0	0	3	43
OC	3	16	0	1	20
UF	3	0	7	3	13
n.e.	0	0	0	14	14
Sum	46	16	7	21	90

Population Response
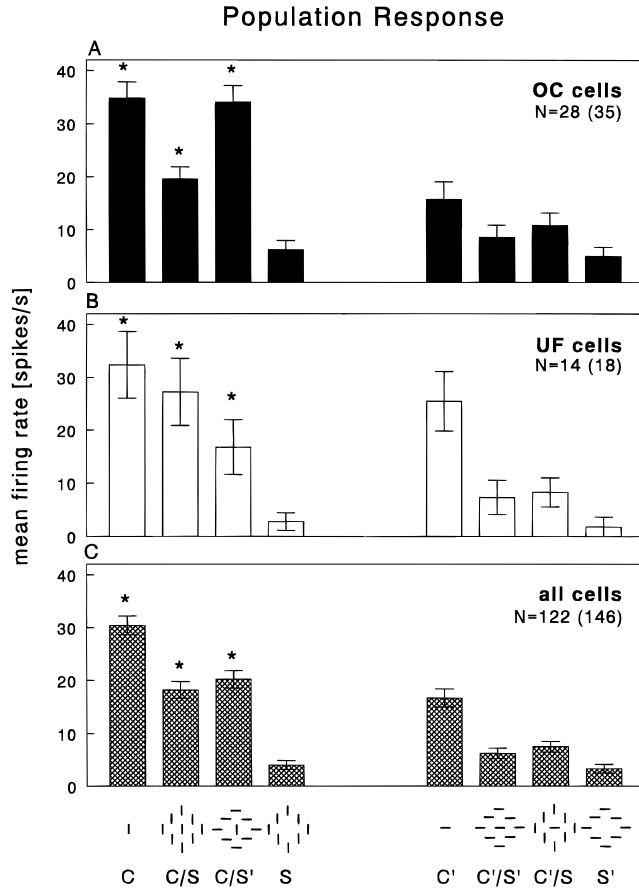
Fig. 4. Mean responses of the entire sample of cells for different texture conditions. In one animal (24 cells), only conditions 1–3 were tested; means that include data from this experiment are marked (*). (A) Means of all OC cells reveal strong suppression from uniform textures (C/S) but little effect in patterns with texture contrast (C/S'). (B) Means of all UF cells show opposite preference (C/S > C/S'); this preference for uniform textures is smaller than that of OC cells for orientation contrast. (C) Means of the entire sample show predominantly general suppression (C/S < C; C/S' < C), with a mild bias for orientation contrast (C/S' > C/S). A similar pattern of results occurs for textures surrounding nonoptimal center lines (right half of graph; C' > C'/S'; C' > C'/S; C'/S > C'/S').

response to a single center line was not affected when orthogonal texels were added in the surround (conditions C/S' *vs.* C), surrounds with texels at the same orientation (condition C/S) produced strong suppression (response reduction by 44% compared to the center line response). There is also a trend for a preference for orientation contrast in the mean responses to patterns around orthogonal center lines (conditions C', C'/S', C'/S) although both texture surrounds evoked suppression here and the difference does not reach significance ($t = 1.84$; $P = 0.076$).

The mean responses of all UF cells are shown in Fig. 4B. Although each cell of this sample showed a reliable preference for uniform texture over the popout condition, the response differences between these conditions are slightly smaller than those for OC cells, but also significant ($t = 4.12$, $P < 0.0001$). Note that the sample does not show the same preference for uniform texture with orthogonal center lines. Here, both texture surrounds produced strong suppression with nonsignificant difference ($t = 0.719$).

The slightly stronger differential effect in OC cells and the higher incidence of such cells predominates when responses are

averaged over all cells (Fig. 4C). Across the entire sample there is considerable suppression from both texture surrounds, with a consistent preference for orientation contrast with either center line orientation. On average, responses to optimal center lines were reduced by 40% and 34% (uniform *vs.* texture contrast), and those to the orthogonal centers by 63% and 55%, respectively. The response differences between texture conditions were significant both for optimal ($t = 2.52$, $P = 0.013$) and orthogonal center lines ($t = 2.36$, $P = 0.020$) despite the inclusion of all UF cells with opposite response preference.

Quantitative analysis of center-surround interactions

Suppression indices

We quantified surround effects by four indices that measure the effect of one or the other surround (S, S') on each of the two center lines (C, C'), using equations of the form

$$SI_{C/S} = (R_C - R_{C/S})/R_C, \qquad (1)$$

where R denotes the cell's response to the specified stimulus condition. The four suppression indices $SI_{C/S}$, $SI_{C/S'}$, $SI_{C'/S}$, and $SI_{C'/S'}$ are positive when the texture surround suppressed the center line response, and negative when the surround produced enhancement.[†] Indices of 0 reveal no effect and indices of 1 complete suppression from texture surround. Values larger than 1 are only obtained if responses were suppressed below the spontaneous firing rate ($R_{C/S} < 0$).

Figs. 5A–5C show the *SI* distributions for optimal center lines. Values obtained for uniform and contrast texture conditions are highly correlated (Fig. 5A), and both distributions are shifted to positive values (Figs. 5B and 5C; one-sample t-test; $t = 10.5$, for $SI_{C/S}$ and $t = 6.27$, for $SI_{C/S'}$; $P < 0.0001$) indicating that texture surrounds predominantly evoked suppression. However, the data points in Fig. 5A are not arranged symmetrically around the oblique axis, as they would be if suppression was equal for both surrounds ($SI_{C/S} = SI_{C/S'}$). Instead the distribution is shifted towards the lower right half of the graph ($SI_{C/S} > SI_{C/S'}$). This is also seen in Fig. 5D which plots the difference of the two suppression indices ($SI_{C/S} - SI_{C/S'}$) for each cell. The distribution (DF_C) is slightly asymmetric, with a bias to positive values. (The shift of the mean is significant at the 0.05 level when a single outlier outside the range of the graph is removed.) This asymmetry is due mainly to the response properties of OC cells (filled circles in Fig. 5A). Interestingly, however, the distribution of *SI* values in Fig. 5A shows no obvious clustering; OC cells do not constitute a distinct group but represent cells on one end of an apparently continuous distribution.

A similar analysis for texture patterns with nonoptimal center lines is shown in Figs. 5E–5H. (As in Table 1, cells whose responses to the orthogonal center line were less than 10% of those to the optimal center were excluded from analysis.) As for optimal

---

[†]In eqn. (1), it is implicitly assumed that texture surrounds themselves do not evoke any response from the cell ($R_S \leq 0$) which was true in only 32% of the cells ($n = 39/122$). For all other cells in which texture surrounds did generate a response, indices might, incorrectly indicate little or no suppression even when responses to full texture patterns were smaller than the sum of responses to individual components, i.e. when surrounds in fact did have a suppressive effect. Thus, indices measured according to eqn. (1) may have *underestimated* the strength of suppression in those cases.

center lines (cf. Figs. 5B and 5C), both *SI* distributions (Figs. 5F and 5G) are shifted towards positive values ($t = 9.21$, for $SI_{C'/S'}$; $t = 6.63$, for $SI_{C'/S}$; $P < 0.0001$) indicating significant suppression by either texture surround. The distribution of *SI* differences (Fig. 5H, $DF_{C'}$) is again slightly asymmetric, but because of the larger scatter of data points in Fig. 5E, this shift is not significant ($t = 0.89$).

Correlations across conditions

As a whole, the *SI* distributions for different texture conditions (Figs. 5B, 5C, 5F, and 5G) look rather similar. This suggested a look for correlations across these conditions. The graphs in Figs. 5A and 5E demonstrate a substantial correlation of *SI* values for *different surrounds* around the same center line. Correlation coefficients are $r = 0.78$ for optimal (Fig. 5A) and $r = 0.70$ for nonoptimal center lines (Fig. 5E) when single outliers outside the graph are removed; the deviations from zero ($=$ no correlation) are highly significant ($t = 15.0$ and $t = 9.05$, respectively; $P < 0.0001$). This indicates that the suppressive effects from different surrounds on the same center line were similar in many cells. The *SI* values for *different center lines*, however, were less strongly related. Correlation coefficients for $SI_{C/S}$ *versus* $SI_{C'/S'}$ (uniform textures) and $SI_{C/S'}$ *versus* $SI_{C'/S}$ (popout conditions) were $r = 0.38$ and $r = 0.26$, respectively ($t = 3.80$ and $t = 2.52$; $P < 0.005$). Suppression effects for different center lines were thus generally less strongly correlated than suppression effects for different surrounds. Interestingly, while *SI*s for uniform textures are highly correlated in OC cells ($r = 0.77$; $t = 5.09$; $P < 0.0001$), *SI*s for popout conditions are not ($r = 0.10$; $t = 0.411$). This indicates that the reduced suppression with orientation contrast seen in these cells often depends on the orientation of the center line. For UF cells, the picture is reversed: *SI*s for uniform textures are not correlated ($r = 0.23$; $t = 0.774$) but *SI*s for popout conditions are ($r = 0.75$; $t = 3.76$; $P < 0.005$). Thus again, the condition with reduced suppression is more variable across center orientations than is the condition evoking the stronger suppression. Both analyses together suggest that reduction of suppression is a more specific phenomenon, and varies more strongly across center lines, than general suppression effects. If this is true, GS cells should show a similarly high correlation for *SI* values both across uniform textures and across popout conditions, as was indeed the case ($r = 0.46$ and $r = 0.54$, respectively; $t = 3.35$ and $t = 4.08$; $P < 0.001$).

Combined and generalized indices

The suppression indices for the different stimulus configurations were combined in order to quantify the major response properties of a cell. For each particular cell, we computed the *general surround effect* (*GSE*) that quantifies the *mean* effect from different texture surrounds, and the *generalized differential firing index* (*GDF*) that quantifies the response *differences* between popout and uniform texture conditions.

Both indices were obtained from associated values for the optimal and the orthogonal center line conditions which were then weighed and averaged across the two conditions. We computed the average suppression index (*ASI*) for a given center line by averaging the suppression indices for the uniform and the contrast texture conditions:

$$ASI_C = (SI_{C/S} + SI_{C/S'})/2, \qquad (2a)$$

$$ASI_{C'} = (SI_{C'/S'} + SI_{C'/S})/2. \qquad (2b)$$

The weighed sum of these values gives the generalized suppression index (*GSI*) which describes the mean suppressive effect of texture surrounds for a given cell:

$$GSI = (R_C \cdot ASI_C + R_{C'} \cdot ASI_{C'})/(R_C + R_{C'}). \qquad (3)$$

In the analysis given here, it is always plotted in sign-reversed form and referred to as the *general surround effect GSE* ($GSE = -GSI$)[‡].

ASI and *GSE* describe the mean modulatory influences of texture surrounds, averaged across different surround types, with no reference to the differential effects that were seen in many cells. These specific modulatory effects were quantified in a second series of indices. We defined an index of differential firing (*DF*) for both optimal and nonoptimal center lines by calculating the response differences between orientation contrast and uniform textures normalized to the response obtained with the same center line alone:

$$DF_C = (R_{C/S'} - R_{C/S})/R_C, \qquad (4a)$$

$$DF_{C'} = (R_{C'/S} - R_{C'/S'})/R_{C'}. \qquad (4b)$$

Together with eqn. (1), this is equivalent to

$$DF_C = SI_{C/S} - SI_{C/S'},$$

$$DF_{C'} = SI_{C'/S'} - SI_{C'/S},$$

as plotted in Figs. 5D and 5H.

The *generalized differential firing index* (*GDF*) (identical to the "differential suppression index" of Knierim & Van Essen, 1992) was then defined as the weighed sum of the differential firing rates for different centers,

$$GDF = (R_C \cdot DF_C + R_{C'} \cdot DF_{C'})/(R_C + R_{C'}). \qquad (5)$$

When comparing the indices for different center lines, averaged suppression (*ASI*) was found to be more strongly correlated than differential effects (*DF*). Correlation coefficients were $r = 0.52$ ($t = 5.67$, $P < 0.001$) for ASI_C *versus* ASI_{C}' and $r = 0.04$ ($t = 0.335$) for DF_C *versus* $DF_{C'}$. This indicates that generally suppressive effects in a cell were little specific and were similarly seen with different center lines, while differential effects often (but not always) occurred specifically for only one orientation. This is consistent with the observation that the classification for differential response categories (OC and UF classes) was less consistent across center lines than the classification for general suppression (GS class, cf. Table 1).

Orientation selectivity

To compare the response properties of a cell with its orientation selectivity, we calculated an orientation selectivity index (*OSI*),

$$OSI = (R_C - R_{C'})/R_C. \qquad (7)$$

The *OSI* is 0 when the cell gave identical responses to the two center line orientations, and 1 when there was no response to the

_____

[‡]This *GSE* is identical to the *GSI* as defined by Knierim and Van Essen (1992).

optimal center line
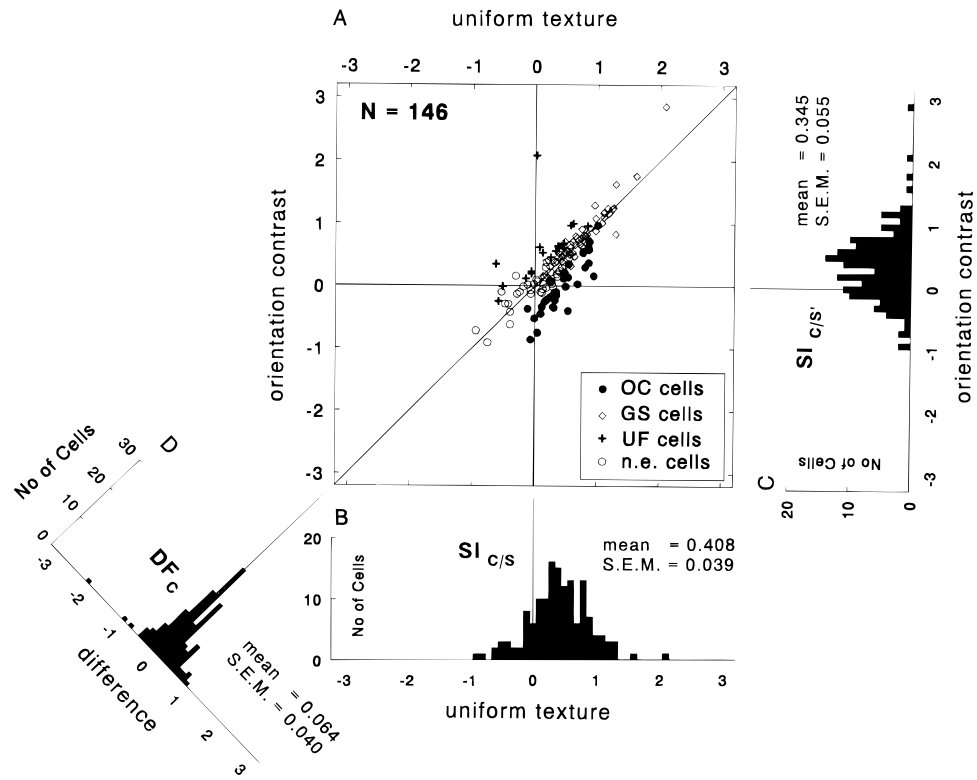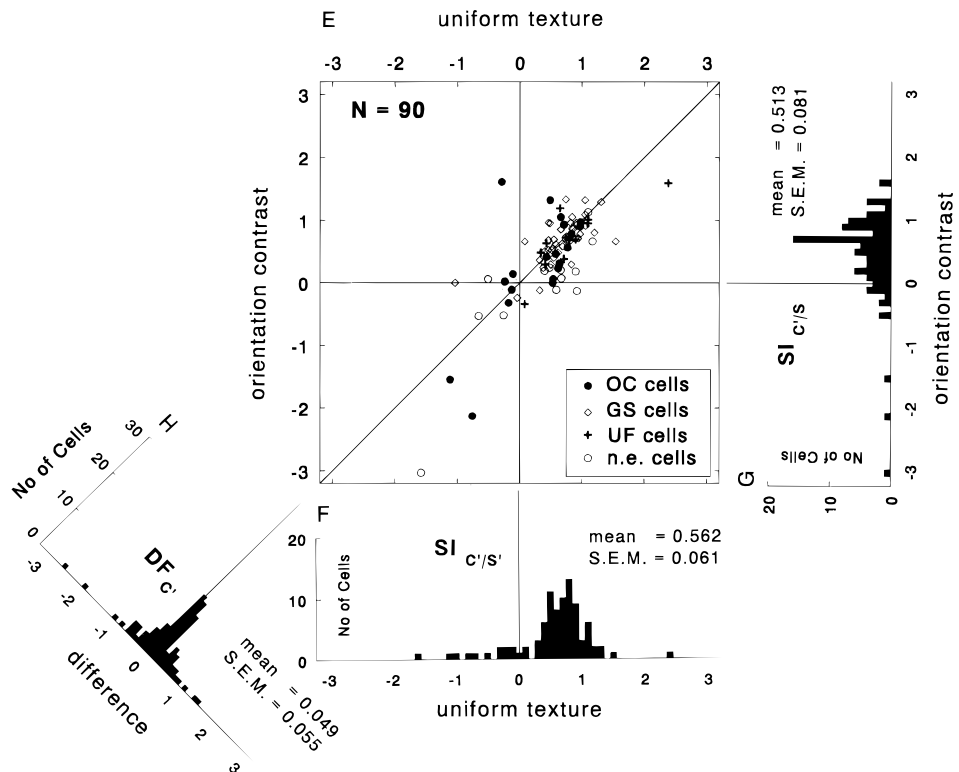

orthogonal center line

FIGURE 5.

orthogonal orientation. The index is greater than 1 when the orthogonal center line suppressed responses below the spontaneous firing rate.

In Figs. 6a and 6b, the general surround effect (*GSE*) and the generalized differential firing rate (*GDF*) are plotted against the orientation selectivity (*OSI*) of each cell. *GSE* values give the mean effect from texture surrounds in a cell. Note that values are plotted differently from the suppression index used before; negative values now indicate a, on average, suppressive effect from texture surround, positive values indicate enhancement. *GDF* values summarize the differential effects of a cell. They are positive for cells that preferred orientation contrast over uniform textures and negative for cells with opposite preference. Note that the *GDF* index does not indicate whether the differential effect was associated with suppression or enhancement of the response by one of the surrounds, or with a combination of both. From Fig. 5, it is however clear that differential responses were often associated with a stronger suppression from uniform textures. In fact, no OC cell showed an enhanced response to such a pattern (no filled circles in the left half of Fig. 5A).

At first glance, the scatter plots in Fig. 6 show little systematic variation of either parameter with *OSI*, except that cells that were on average enhanced by texture surrounds (*GSE* > 0) tended to be orientation selective. Many of these neurons were OC cells (filled circles); only one enhanced UF cell was found (crosses). While OC cells displayed a large range of orientation selectivity, several cells being highly selective with an *OSI* near 1 UF cells were generally less orientation selective. In the whole-cell sample, neither general suppression (negative *GSE* values) nor differential firing (positive *GDF* values) was closely linked to the orientation selectivity of a cell ($r = 0.26$ for *GSE*; $t = 2.88$, $P < 0.005$; $r = 0.19$ for *GDF*; $t = 2.09$, $P < 0.05$), in agreement with Lamme (1995). Significant correlations were only seen in the subsample of OC cells (filled circles; $r = 0.31$ for *GSE*; $t = 2.49$, $P < 0.01$; $r = 0.62$ for *GDF*, $t = 3.98$, $P < 0.001$); for all other classes correlations were non-significant ($t < 1.6$, $P > 0.1$). Thus, orientation-selective OC cells produced stronger response differences between uniform texture and the popout condition than orientation nonselective OC cells. However, this cannot be generalized to all cells, since many orientation-selective cells did not belong to the OC class and produced no significant response differences with these patterns (cf. the open symbols in Fig. 6b). The correlation in Fig. 6a is likely related to that in Fig. 6b. If orientation-selective OC cells tend to have a large *GDF* (cf. Fig. 6b), their responses to the different surround conditions must differ considerably. Hence, their *GSE* (for which the effects from all texture surrounds are averaged) cannot be very low and may instead even be positive. Non-

selective OC cells, on the other hand, would express small differences between surround conditions (low *GDF*; cf. Fig. 6b); they could have positive *GSE* only if being generally enhanced by any texture surround. Such a response property, however, was very rarely seen.

In Figs. 6c and 6d, these data are plotted in histogram form. The *GSE* values (Fig. 6c) are shifted towards negative values (one-sample *t*-test; $t = 8.85$; $P < 0.0001$), indicating suppression by the texture surround. This shift was significant in GS cells ($t = 16.3$; $P < 0.0001$; open rhomboids in Fig. 6a) and UF cells ($t = 4.70$; $P < 0.0001$; crosses in Fig. 6a), but not in OC or n.e. cells. The distribution of *GSE* values for the entire sample (Fig. 6d) is nearly symmetric around a mean of -0.42; that is, texture surrounds suppressed the responses to single lines by an average of 42%.
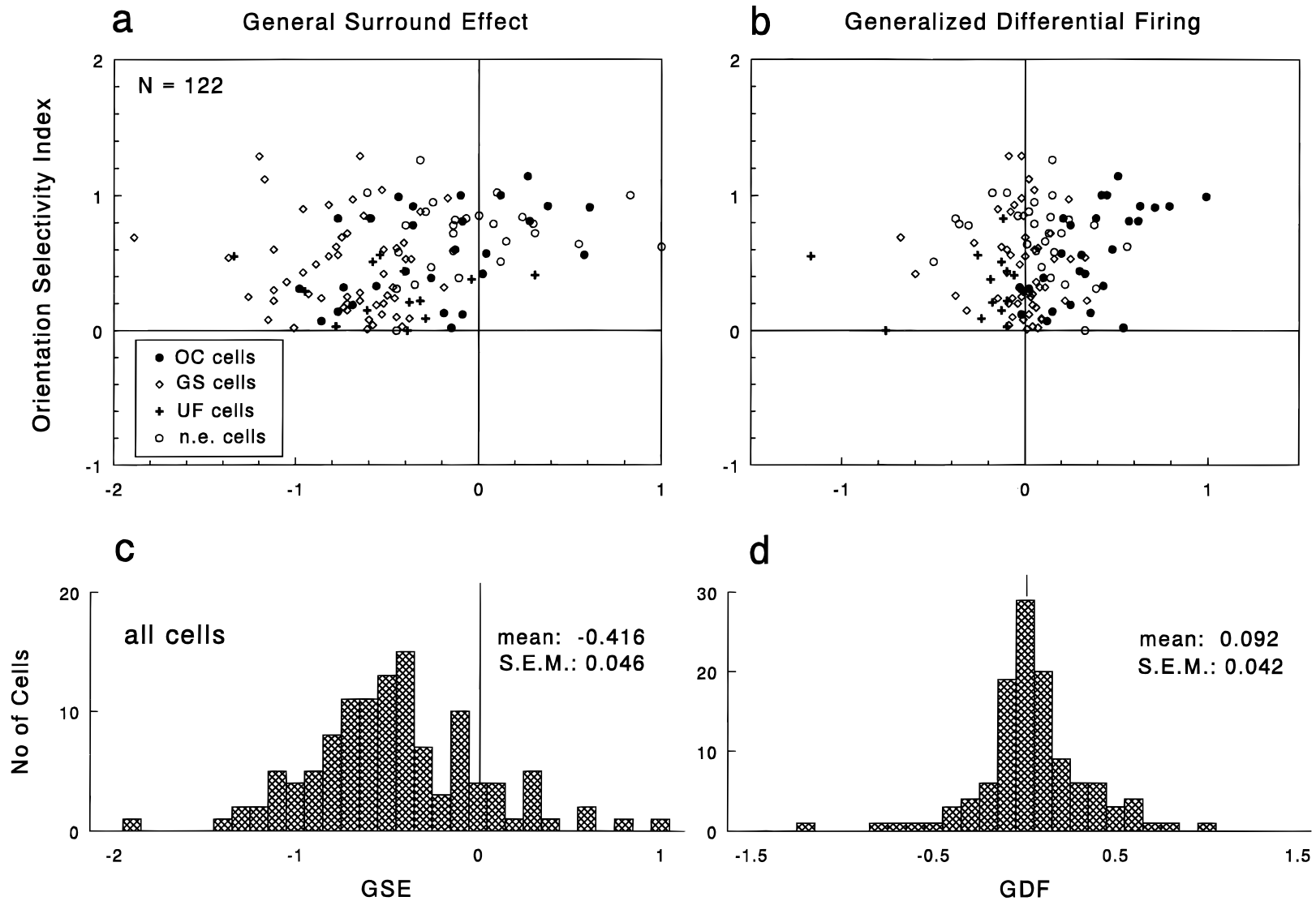
Differential effects (Fig. 6d) were naturally not consistent across cell groups. *GDF* distributions for OC cells (filled circles in Fig. 6b) were shifted towards positive values ($t = 3.47$; $P < 0.001$) and those for UF cells (crosses in Fig. 6b) towards negative values ($t = 2.99$; $P < 0.005$). Because of the larger number of OC cells and the generally stronger differential effects they showed, the *GDF* distribution of the total cell sample was significantly ($t = 2.10$; $P < 0.05$) shifted towards positive values, indicating a global preference for orientation contrast. No significant shifts were seen for GS or n.e. cells.

The analysis above gives a consistent picture of texture modulation in V1 under anesthesia. Texture surrounds evoked considerable suppression of the responses to single lines over the RF. In a large proportion of cells, different surrounds produced different effects, often a preference for orientation contrast. To elucidate the neuronal mechanism underlying these effects, several response properties were analyzed in more detail. In the following sections, we analyze the temporal properties of center-surround interactions, the variation of response properties with texture density, and the distribution of effects across cortical layers.

Time scale of interaction

While the analysis above was based on firing averaged over the full period of stimulus presentation, we also saw interesting variations in the time course of responses to different texture patterns. For example, Fig. 7 shows superimposed the response histograms of a generally suppressed cell for the center line alone and for the two texture conditions with this line. Both texture surrounds evoked strong suppression, but in the popout condition (C/S′) suppression was slightly reduced during the latter part of the response (*ca.* 65–95 ms after stimulus onset).

Fig. 5. Suppression indices (*SI*) for patterns around optimally oriented and orthogonal center lines. (A) Scatter plot of *SI* for uniform textures *versus SI* for orientation contrast, with optimal center lines. Each point represents one cell. Cells were classified as GS, general suppression by either texture surround; OC, preference for orientation contrast; and UF, preference for uniform texture. Cells with no significant effect are also shown (n.e.). Suppression indices for different patterns are correlated ($r = 0.78$) with a slight shift to the lower right half of the plot (OC cells). (B) Distribution of *SI* values for uniform and (C) orientation contrast conditions. Both distributions are shifted to positive values indicating suppression from texture surround. (D) Distribution of differential firing rates, $SI_{C/S} - SI_{C/S'}$. The mean is shifted to positive values (preference for orientation contrast). (E–H) Suppression indices for patterns around orthogonal center lines plotted in similar diagrams as in (A–D). Data from cells whose responses to orthogonal lines were less than 10% of the responses to the optimal center lines are not included. Same categories as in (A), that is, cells were classified on the basis of their responses to textures with optimal center lines. Scatter plot and distributions display the same characteristics as in (A–D) except that all categories are intermixed. *SI* values for uniform texture and for orientation contrast are correlated ($r = 0.70$, E) and both distributions are shifted to positive values (F, G).

a General Surround Effect

N = 122

● OC cells
◇ GS cells
+ UF cells
○ n.e. cells

Orientation Selectivity Index

b Generalized Differential Firing

c

all cells

mean: -0.416
S.E.M.: 0.046

No of Cells

GSE

d

mean: 0.092
S.E.M.: 0.042

GDF

Fig. 6. The major modulatory effects plotted against the orientation selectivity of each cell. (a) General surround effects (*GSE*, negative values indicate suppression, positive values enhancement); (b) generalized differential firing rates (*GDF*, positive values indicate preference for texture contrast, negative values preference for uniform texture). Neither index is strictly correlated with the strength of orientation tuning of a particular cell, although enhancement effects (*GSE* > 0) were only seen in orientation-selective cells. Response categories are independent of orientation tuning. *Within* the OC category, however, the strength of differential effects is related to orientation selectivity. (c,d) Distributions of data points in (a) and (b) are significantly shifted to general suppression (c) and preference for orientation contrast (d).
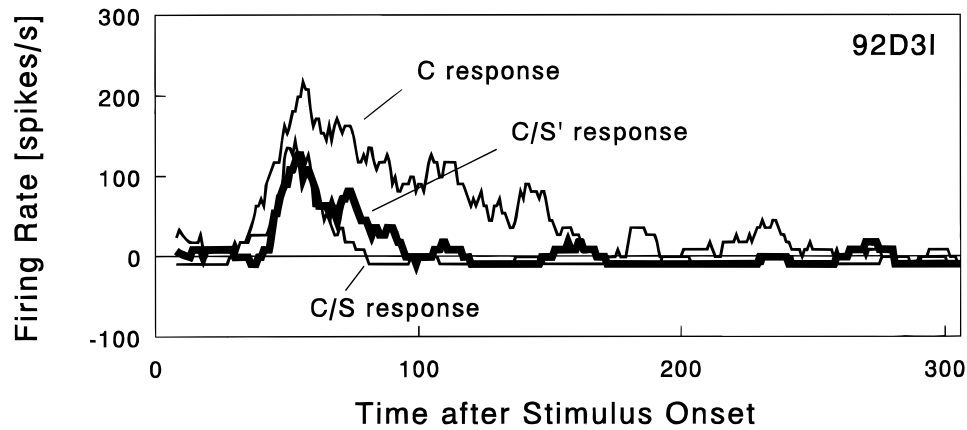
Fig. 7. Delayed differences of surround effects. Responses of a single cell to the optimally oriented center line (C) alone and in different texture patterns (C/S, C/S′). Both texture surrounds evoked strong suppression. But while the responses to the texture conditions were similar during the first 60 ms after stimulus onset, they strongly differed thereafter. Histograms (binwidth 1 ms) are smoothed with a 7-ms rectangular window for better visibility.

To evaluate the time course of surround effects in V1, we computed mean peri-stimulus time histograms (PSTHs) from all cells that had both a significant surround effect and a brisk response to the center line (Fig. 8). Initially both texture surrounds produced similar levels of suppression beginning at the onset of the excitatory response (C *vs.* C/S and C/S′ curves; arrow downward). Later responses to the two texture surrounds diverged, producing a weaker differential response (C/S *vs.* C/S′ curves; arrow upward). These two effects can be distinguished best in separate averages of cells from different categories. Mean responses are shown in Fig. 8B; differences of these curves are plotted in Fig. 8C.

Response latencies

According to Fig. 8B, response latencies varied across cell classes. The earliest responses were seen in GS cells, perhaps due to a number of layer 4C cells with brisk responses that were included in this group. Responses of UF cells were only marginally slower. OC cells, on the other hand, responded later than both GS and UF cells. The later response of OC cells was just about significant when latencies of individual cells are compared (independent *t*-test; $t = 2.42$ for OC *vs.* GS; $t = 2.10$ for OC *vs.* UF; $P < 0.05$); latency differences between the GS and UF class were not significant ($t = 0.393$). Responses to patterns with texture surround were generally delayed compared to responses to the center lines alone. These differences were small across the cell sample [49.7 (C) *vs.* 54.5 (C/S) and 53.3 ms (C/S′), respectively] but reliable (paired *t*-test; $t = 2.64$ (C *vs.* C/S) and $t = 3.63$ (C *vs.* C/S′), $P < 0.01$). Differential effects occurred with a latency of about 60 ms in both OC and UF cells. About 15–25 ms elapsed between the earliest responses in V1 and the onset of differential effects.

General suppression

Suppression in GS cells began at response onset (downward arrows in Fig. 8B; short dashed lines in Fig. 8C) and continued throughout the entire response period. General suppression increased quickly and reached its maximum within 70 ms, at or even before the time of the response peak (compare response differences between conditions C and C/S, or C/S′, thin curves in Fig. 8C). In

OC cells, responses were also suppressed at response onset, but differences between single lines and texture patterns increased more slowly than in GS cells, and reached their maxima 80–90 ms after stimulus onset. General suppression then decayed relatively fast (up to 150–200 ms after stimulus onset). In UF cells, general suppression was absent until the onset of differential effects.

Differential effects

Response differences for texture contrast versus uniform texture developed about 60 ms after stimulus onset (arrows upwards in Fig. 8B; continuous straight lines in Fig. 8C). They were negligible in GS cells but had a similar time course (though opposite sign) in OC and UF cells (Fig. 8C, thick curves). Response differences increased continuously up to about 100 ms after stimulus onset, and remained nearly constant thereafter. Note that early responses of OC cells to orientation contrast were suppressed relative to the center line response (thick *vs.* thin continuous curves in Fig. 8B, OC cells) but later exceeded that response. This was not seen in UF cells.

We applied the following test to establish the different onset of general and differential effects on statistical grounds. For each cell, responses were taken from small time windows (30 ms) before and after the onset of differential effects (based on Figs. 8B and 8C, this value was arbitrarily set to 60 ms). Responses in these windows were then compared across test conditions and the reliability of differences within a cell class was established using paired *t*-test analysis. For the GS cells (Fig. 8B, upper graph), response differences between the C condition and either C/S or C/S′ were significant in both time windows (interval 31–60 ms: $t = 4.37$ for C *vs.* C/S, $t = 4.56$ for C *vs.* C/S′; $P < 0.0001$; interval 61–90 ms: $t = 6.21$ for C *vs.* C/S, $t = 6.46$ for C *vs.* C/S′; $P < 0.0001$); the differences between texture conditions were not significant (C/S *vs.* C/S′: $t = 0.927$ for 31–60 ms, $t = -0.868$ for 60–90 ms). For the OC cells (middle graph), response differences between the single line and the full texture conditions were significant before 60 ms (interval 31–60 ms: $t = 4.15$ for C *vs.* C/S, $t = 3.57$ for C *vs.* C/S′; $P < 0.005$) but not the differences between the texture conditions themselves (C/S *vs.* C/S′: $t = -1.05$). After 60 ms, however, all differences became significant (interval 61–90 ms: $t =$
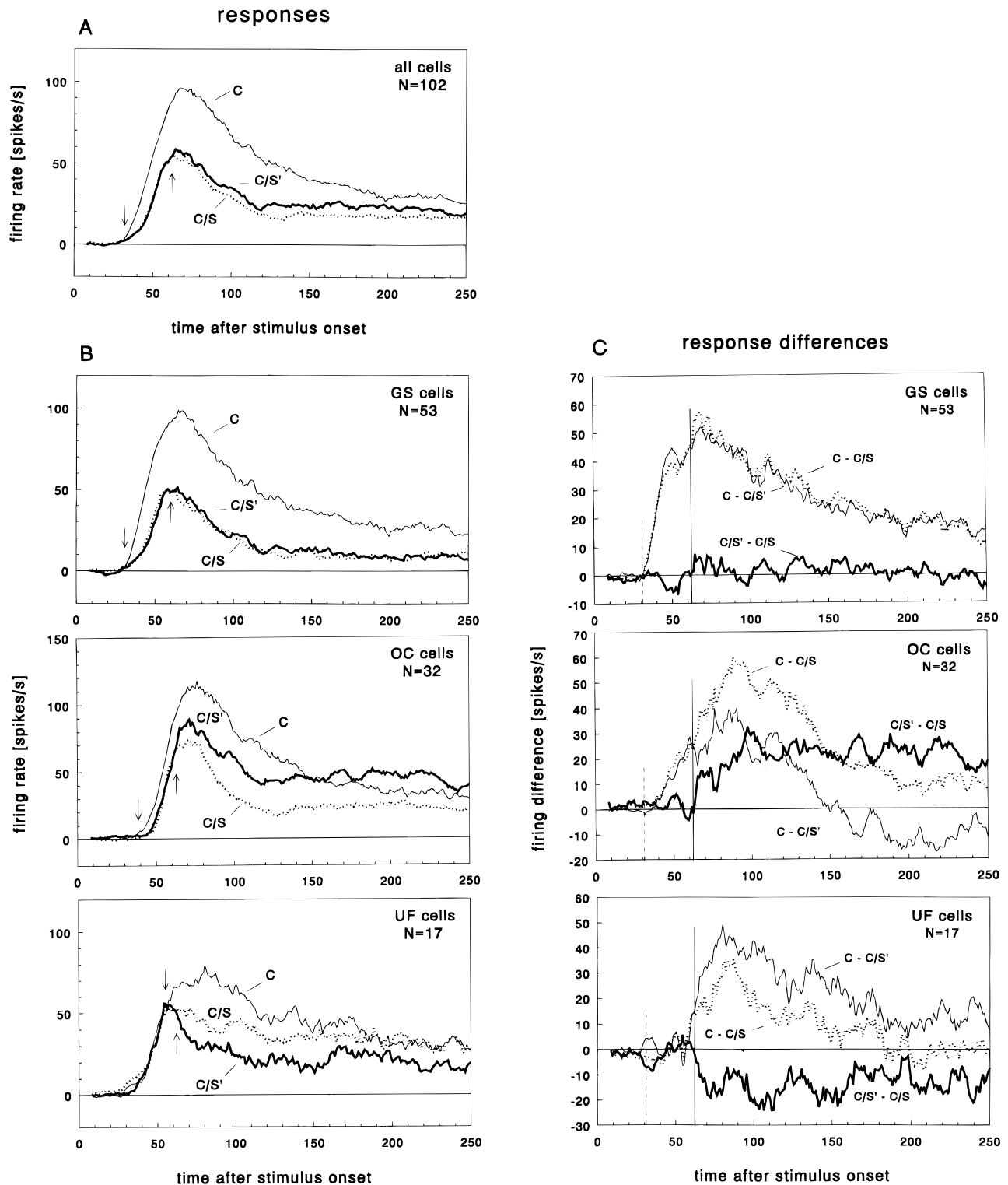
Fig. 8. Mean responses and response differences to the different texture conditions. (A) Histogram of the mean response of all cells that showed a significant surround effect and gave a sufficiently brisk response to the center line alone. Responses are smoothed (11-ms rectangular window) for clarity. (B) Response histograms of cells from different subgroups. Mean responses to optimal center lines alone (C) or with either texture surround (C/S; C/S′) are superimposed. Onsets of generally suppressive and differential effects are marked by downward and upward pointing arrows, respectively. (C) Response differences for the cell groups in (B). Long vertical lines mark the onset of differential effects from texture surround; short (dashed) lines mark the onset of general suppression in GS cells. Except for UF cells, general and differential effects have different latencies. All marks (arrows, vertical lines) are adjusted by hand for best visual fit; in (C) the same line position was used for all graphs.

6.95 for C *vs.* C/S, $t = 7.02$ for C *vs.* C/S′; $P < 0.0001$; $t = -2.91$ for C/S *vs.* C/S′; $P < 0.01$). Among the UF cells (lower graph), finally, there were no significant differences between the different test patterns in the time window before 60 ms (interval 31–60 ms: $t = -0.244$ for C *vs.* C/S, $t = -0.144$ for C *vs.* C/S′, $t = 0.035$ for C/S *vs.* C/S′) but all differences were significant in the window thereafter (interval 61–90 ms: $t = 3.01$ for C *vs.* C/S, $P < 0.01$; $t = 4.99$ for C *vs.* C/S′, $P < 0.0005$; $t = 2.73$ for C/S *vs.* C/S′, $P < 0.05$).

We conclude that (1) texture surrounds generally increased the latency of responses in GS and OC (but not UF) cells, probably because of the strong suppression often evoked from texture surrounds, that (2) general suppression and differential effects (in GS and OC cells) occurred with different latencies, differential effects were significantly delayed, and that (3) UF cells appeared to lack any early generally suppressive effects. Fig. 8C also showed that differential effects were sustained for the duration of the stimuli. Though effects were complementary in OC and UF cells, they seemed to follow the same time course in both cell classes.

The spatial range of contextual effects

An important aspect of center-surround interactions in V1 is the spatial range over which texels in the surround can modulate responses. We analyzed the effects of texture scale and spacing in 17 cells, including three OC cells, by varying the spacing of the texture grid or the magnification of the whole texture pattern. Both manipulations affected the spacing of texels in the surround as well as the distance of the nearest texels to the center line. General surround effects tended to diminish as texel spacing increased (Fig. 9A) and the strength of general suppression usually decreased. Also differential effects diminished in strength when raster width was increased (Fig. 9B) but this trend was less pronounced in some cells. The spatial range of surround effects varied widely across cells, both in terms of relative spacings (normalized to RF size) and absolute spacings (in deg) as plotted here. However, sample means show a clear trend of decreasing general suppression with increased spacing but no net differential effect (Fig. 9C).

Fig. 9D plots the *GSE* values of all seven GS cells in this sample. Suppression always diminished with increasing spacing. If the spatial extent of texture suppression were fixed, then the curves should lie on top of one another. But they do not, even not when line spacing is normalized to the RF size or to the size of the texture elements. This suggests that the spatial extent of texture suppression varies from cell to cell.

Fig. 9E shows the *GDF* values of the three OC cells of this sample, plus data from two other cells that were classified as GS and n.e., respectively, with our standard test but revealed a preference for orientation contrast with larger texture spacing. The *GDF* values did not always decrease with increased spacing. However, when compared with the *GSE* values from the same sample, both differential and general effects disappeared at the largest texture spacings tested (Fig. 9F), suggesting that both effects have a similar spatial range.

These data clearly show that texture density influences the magnitude of the modulatory effects of texture surrounds. Interactions decreased with increased texel spacing and virtually disappeared with spacings larger 2 deg. With the range of line lengths used for these cells (0.4–1.3 deg; mean: 0.6 deg), the spatial range over which surround effects were seen was about 3–4-fold, which is on the same order as predictions from psychophysics (Nothdurft, 1985*b*).

Depth analysis

To permit analysis of responses in terms of cortical layers, we made long electrode penetrations while recording from as many neurons as possible. Unfortunately, tissue sections were not available for histological analysis, so we related response properties of cells to the recording depth estimated from landmarks obtained during electrophysiological recording (depth of first neuronal activity, depth of first white matter responses, or sudden shifts in RF position). The relative depth of recorded cells was normalized to this scale. This normalization was done in order to account for possible variations in the length of different penetrations, either due to variations in cortical thickness or due to possible tilt of the recording electrode. Cells encountered in penetrations in which these landmarks could not reliably be localized and cells encountered in deeper cortical folds of V1 were not included in the analysis.

A sample of 67 cells from eight electrode penetrations through the striate cortex were selected for analysis using these criteria. Response properties of this sample are plotted against recording depth in Fig. 10. Recording depth between landmarks was divided into ten slices of equal thickness. Slice 1 corresponds to superficial layers and slice 10 to the deepest layers. The number of cells encountered within each slice is shown in the top panel of Fig. 10. The uppermost and lowermost depth slices contain relatively few cells, but the remaining slices contain a sufficient number of cells for analysis.

The graphs below show mean values of general (*GSE*) and differential surround effects (*GDF*) of cells within each depth slice. (For 13 cells, modulation was only tested for optimal center lines and these values instead of the generalized ones were used.) General suppression was pronounced at all recording depths giving mean values that are indistinguishable across layers (ANOVA; $F_{9,57} = 0.5$, $P = 0.87$). *GDF* data reveal a general preference for orientation contrast in all slices except 5, 6, and 10, where negative values indicate some preference for uniform textures. The preference for orientation contrast was particularly strong in slice 7. These differences are reliable ($F_{9,57} = 2.16$, $P = 0.039$), in particular when slices 1–4 are pooled and also slices 8–10 ($F_{4,62} = 4.59$; $P = 0.0026$). The different distributions in Fig. 10 suggest that all layers contribute comparably to general surround effects, but that differential responses may vary in strength in different subsets of layers.

To relate this analysis to the categorization of response properties presented earlier, the proportion of OC and UF cells in each depth slice is plotted in the bottom panels of Fig. 10. Values are given as percentages of the number of cells within each slice (upper panel). Although the analysis is based on a small number of cells and must be interpreted with care, cell classes were apparently not evenly distributed across slices. OC cells occurred above and below slice 5 but not within it, and were most frequent in slices 3 and 7. In contrast, the distribution of UF cells appears to be unimodal with a peak at depth slice 6. These distributions were consistent with the variation of *GDF* values across cortical slices (third panel).

Discussion

Our experiments demonstrated pronounced modulatory effects from visually unresponsive areas outside the classical RF in anesthetized animals. These effects were primarily, but not exclusively suppressive, and often depended on the relative orientation of lines in the center versus the texture surround. Texels at the same ori-
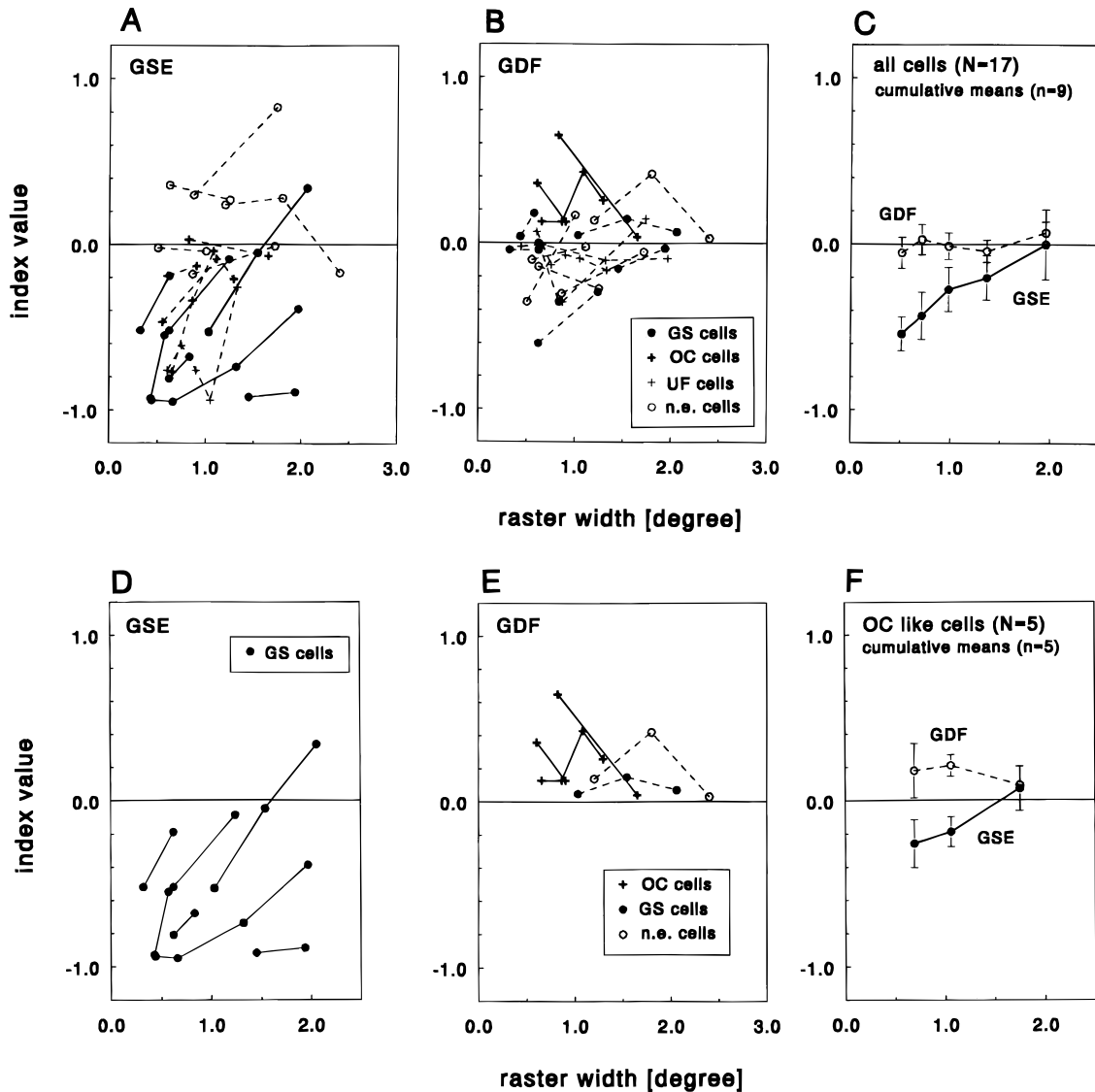
Fig. 9. The spatial range of modulatory effects from texture surround. Data show general suppression effects (*GSE*) and generalized differential firing rates (*GDF*) of 17 cells that were tested with multiple raster widths. Values are plotted against the effective spacing of texture elements (in degree of visual angle) whether that resulted from true variations of the spacing of otherwise identical texture elements or from scale variations of the whole pattern. (A) *GSE*, and (B) *GDF* data of all 17 cells classified according to their responses to textures with standard raster widths (inset in B). Data points from the same cell are connected by a line. (C) Cumulative means of data points in (A) and (B) averaged over *n* adjacent values with increasing raster widths. While the general suppression decreases continuously with increasing raster width, no net differential effect is seen in this sample. (D–E) Selected plots of subgroups in (A) and (B); (D) all GS cells and (E) all OC cells plus two cells with differential effects at a larger raster width. For each individual cell in (D), the general surround effect diminishes with increasing raster width, but the spatial extent and strength of the effect differ considerably between cells. Differential effects in (E) are less systematic but are also generally reduced with larger raster widths. (F) Cumulative plots of data points in (E) and the corresponding *GSE* values. Curves suggest a similar spatial range of these effects.

entation as the center line generally suppressed the center response more strongly than texels at the orthogonal orientation.

Several properties of the observed modulatory effects suggest that they can be looked at as a combination of two phenomena: nonspecific general suppression, and specific differential effects. First, general suppression had a shorter latency than did differential effects (Fig. 8). Second, general suppression was often similar for different center lines, whereas differential effects could vary considerably with center line orientation (Table 1 and Fig. 5). Third, general suppression was observed in all layers, whereas the various differential effects tended to be less uniformly distributed (Fig. 10).

Relation to earlier studies

Our data obtained in anesthetized animals are similar to those described for the alert monkey (Knierim & Van Essen, 1992). With similar stimuli as ours, these authors reported the same major response properties, although with a slightly different distribution: they found fewer GS cells (27% compared to 41% in our sample when classification was made according to their scheme), fewer UF cells (6% *vs.* 11%), and more OC cells (32% *vs.* 26%). The additional categories they reported were based on response differences between the two center lines. We did not apply this distinc-

tion here because of the relative rarity of such cells and because of the difficulty in classifying cells that do not respond to nonoptimal center lines. Given the variation of response properties with different center lines (cf. Table 1), we doubt that further subdivisions of the major response classes would aid in understanding the underlying mechanisms.

Depth Analysis

The general similarity of effects seen in both studies suggests that contextual modulation at V1 is largely preserved under the levels of sufentanil anesthesia used in the present study. However, the number of cells with preference for orientation contrast was smaller than in the alert animal, and the number of UF cells was increased. As a consequence, population responses to uniform textures and popout patterns were less distinct than in the data of Knierim and Van Essen, but a general preference for orientation contrast was still significant. Thus, there may be modest effects of sufentanil anesthesia on quantitative aspects of surround modulation, and even larger effects using different anesthetics or anesthesia levels (Zipser et al., 1997). In this regard, it is relevant that the percentage of OC cells in our study is similar to that found in cats under nitrous oxide and pentobarbiturate anesthesia (Kastner, Nothdurft, & Pigarev, submitted). These authors found 22% OC cells using our classification scheme, compared to 24% in the present study. Despite these differences on quantitative ground, however, it is important to note that the type of effects did not differ between the studies and that all major properties of contextual modulation seen in the alert animal were also found in the anesthetized preparation. In particular with regard to temporal properties, we confirmed Knierim and Van Essen's (1992) observation that the onset of differential effects is significantly delayed relative to general suppression in OC cells. However, Knierim and Van Essen did not report the different onset of general suppression in OC and UF cells that was seen in our cell sample.

Several studies in anesthetized cats have reported contextual modulation by stimuli outside the classical RF, and many of these have found specific surround effects qualitatively similar to those reported here (Blakemore & Tobin 1972; Bishop et al., 1973; Maffei & Fiorentini, 1976; Fries et al., 1977; Kato et al., 1978; Nelson & Frost, 1978; Orban et al., 1979; Albus & Fries, 1980). Taken together these data suggest that there are few if any systematic differences between the modulatory effects occurring in cats and monkeys. Gilbert and Wiesel (1990) analyzed the orientation tuning of the surround and reported a predominance of cells with properties similar to the UF cells in our study, which we observed predominantly in middle layers and which, among the whole sample and across all layers, were, in fact, less frequent than OC cells. Other studies found mainly neurons for which response suppression was strongest when stimuli in the surround matched the orientation of stimuli in the RF, consistent with the response properties of our OC class (De Angelis et al., 1994; Li & Li, 1994; Kastner et al., 1997). DeAngelis et al. (1994) suggested that non-
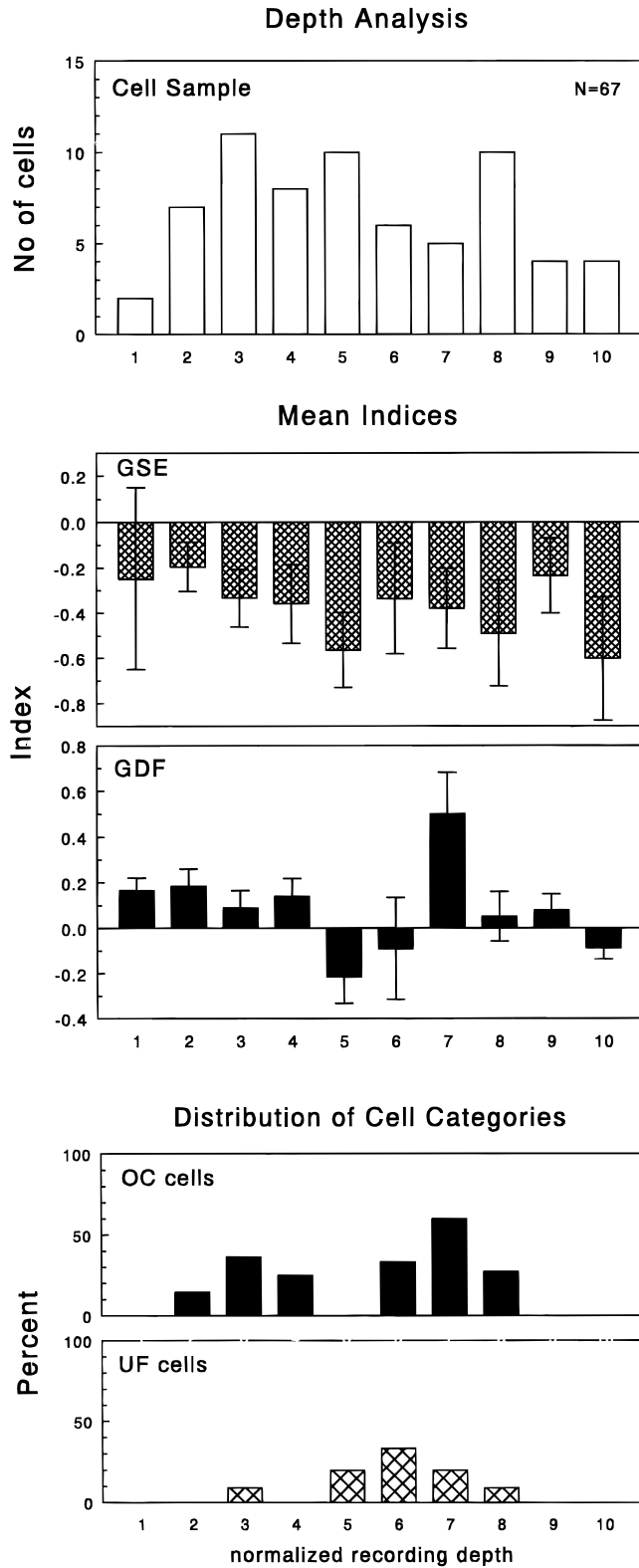
Fig. 10. Analysis of response properties of 67 cells with reconstructed recording sites. In each panel the physical distance between the location of the first neural activity encountered in a penetration and the first activity indicating the presence of white matter is divided into ten equal slices. Slice 1 refers to superficial and slice 10 to deep layers of striate cortex. The numbers of cells encountered in each slice are plotted on top, the mean values of two indices within slices below (*GSE*, general surround effect; *GDF*, generalized differential firing rate). Preference for orientation contrast was greatest in slice 7 but is also seen in most other slices (except 5, 6, and 10). General suppression was observed in all cortical layers. The bottom panels plot the distribution of cell categories within depth slices (normalized to the number of cells in each slice). Orientation contrast (OC) cells appear to be distributed bimodally and to spare the presumed thalamic input layer (slice 5). The distribution of UF cells, with preference for uniform texture patterns, was nearly unimodal with a maximum at depth slice 6.

specific suppression, in the cat, may arise from stimuli impinging on the classical RF, whereas stimuli outside the RF would always produce differential effects. Though we cannot rule out this possibility completely, it seems unlikely to account fully for our results in the monkey, particularly for cells showing strong general suppression with surround stimuli that elicited no direct response (signifying little or no encroachment on the classical RF) and that consisted of long narrow texels having little Fourier energy in the orthogonal orientation. Moreover, we found both specific (differential) and nonspecific (general) effects over the same range of texel spacings. Suppression was maximal at or near the border of the RF and continuously decreased with increased texel spacing up to distances of more than 2 deg (Fig. 9), far beyond the boundary of the excitatory RF. Nevertheless, the fact that we used bars, not gratings in the surround, implies that for any texel orientation the orthogonal component is not zero. In particular for wider texels, therefore, both optimal and orthogonal surrounds could have activated the same neuronal mechanisms. Differential effects could then be hidden in the responses to such stimuli, compared to gratings, and apparent general suppression might have become predominant. (Note that this would not account for differences between Knierim & Van Essen's data and ours, since both studies were done on monkeys and in both studies surrounds with bars, not gratings, were used.) While these effects might have affected our classification to some extent, we doubt that they could account for all the many GS cells we have seen. We have generally used rather small texels, with an averaged width of 0.09 deg (less than 6 min of arc).

Sillito and colleagues (Sillito et al., 1995) recently reported effects in both cat and monkey that were similar to those reported here. They found differential responses to uniform patterns and patterns with orientation contrast, and these differential responses did often not depend on the absolute orientation of the center stimulus. They also demonstrated pronounced facilitatory effects of the texture surround (also see Maffei & Fiorentini, 1976). We, too, have seen facilitation from orientation contrast in some cells (e.g. Fig. 3a; cf. data points below midline in Fig. 5A). These effects were, in fact, strong enough to compensate the suppression found in other cells (e.g. Fig. 3b) so that the mean response of OC cells in the population was unaffected by orientation contrast (Fig. 4A). However, strong facilitatory effects from texture surround were relatively rare in our cell sample (cf. Fig. 5A, *SI* values < 0) and far less frequent than suppressive effects. The predominant modulatory effect of texture surrounds was suppression, in agreement with Sillito et al. (1995) and earlier studies in the monkey (e.g. Born & Tootell, 1991).

Preference for orientation contrast in area V1 was also observed by Lamme (1995) and Zipser et al. (1996). They found that texture patches embedded in a contrasting surround often evoked larger responses than those same patches embedded in a large uniform field. As in our experiments, these response differences were only apparent after some delay, though latencies were slightly shorter in our study than in theirs. Interestingly, similar responses were observed when targets were defined by dimensions other than orientation (Lamme, 1995; Zipser et al., 1996), supporting the general importance of contextual modulation in V1 (cf. Allman et al., 1985, 1990; Li & Li, 1994; Kastner et al., 1997).

Neuronal mechanisms

While general suppression clearly resembles an inhibitory effect, the basis of differential firing is not as obvious. In spite of the pronounced suppressive effects, it is natural to assume that differ-

ential effects are due to stronger suppression from texels in the surround at the same orientation as that of the center line (iso-orientation inhibition). But facilitatory effects in some cells and the observation that late responses to texture contrast could exceed the center responses (cf. Fig. 8) suggests that the increased responses to orientation contrast might also be caused by specific (cross-orientational) disinhibition of nonspecific suppression.

Although our experiments suggest two types of texture modulation, it is likely that several neural mechanisms contribute to these results. These include subcortical mechanisms like center-surround interactions in geniculate cells; long-range horizontal or local circuit interactions within area V1; and feedback from higher cortical areas.

Subcortical effects

General suppression may arise partly from center-surround interactions in the retina or the LGN, as we observed in occasional recordings from LGN fibers in this study. However, subcortical mechanisms cannot explain the often pronounced differential effects with the different texture surrounds. Even when such effects were seen at the geniculate level they appeared to be cortical in origin (Sillito et al., 1993).

Interactions within V1

Inhibitory effects from regions outside the RF were originally linked to inhibitory endzones and inhibitory sidebands. Interactions were found to be orientation specific, and strongest for lines at the cell's preferred orientation (iso-orientation inhibition; Orban et al., 1979). Recent studies, however, suggest that these effects are not restricted to endzones and sidebands but are a general property of the surround (De Angelis et al., 1994; Li & Li, 1994). The differential effects we have observed appear to be consistent with this view (see Knierim & Van Essen, 1992).

Long horizontal connections in the striate cortex may partially account for the spatial extent of texture surround modulation. These connections may extend over 6–8 mm of cortex (Gilbert & Wiesel, 1989) and preferentially link neurons with similar orientation preferences (Ts'o et al., 1986; Ts'o & Gilbert, 1988). Although these connections themselves are excitatory, they terminate on excitatory cells and inhibitory interneurons (McGuire et al., 1991) and could thus potentially produce the specific suppression we have seen. Long-range interconnections are found predominantly in layers 2 + 3 in the macaque (Rockland & Lund, 1983) but may also modulate units in infragranular layers *via* local cortical circuitry. Thus, these connections could potentially account for most of the properties of OC cells that we have seen. However, our data also demonstrate that surround suppression was partially dependent on the actual orientation of the center line. It is not immediately obvious how long-range cortical connections between similar orientation columns could produce this effect.

Feedback

Also feedback from extrastriate areas into V1 may contribute to contextual modulation, as suggested from a recent lesion study by Lamme et al. (1997). The properties of feedback connections may account for several aspects of our results. For example, the latency differences we found between general and differential suppression could result from the different latencies of feedback as compared to feedforward effects. Feedback projections terminate mainly in supragranular and infragranular layers of the preceding area (Maunsell & Van Essen, 1983; Rockland & Virga, 1989; Felleman & Van Essen, 1991) but spare layer 4. So, the preference for orientation

contrast should be strongest in layers above or below layer 4 and absent from layer 4 itself, consistent with our data (Fig. 10, bottom panels) and with the location of feature contrast response components in supragranular and infragranular layers of the primary visual cortex (Lamme et al., 1993*a*,*b*, 1994). Finally, feedback connections could modulate responses from regions outside the classical RF, by virtue of the larger receptive fields of cells at higher stages of visual processing. Suppressive feedback from cells with similar orientation preference could then produce the increased suppression in uniform texture fields, a basic aspect of differential effects in our data. The fact that similar modulatory effects have been observed in V1 across a wide variety of dimensions (orientation, motion, luminance, color, and depth; Lamme, 1995; Zipser et al., 1996), some of which are at least partly analyzed in higher areas, seems to support the role of feedback connections in contextual modulation.

Texture processing in area V1

The majority of V1 cells were suppressed by large texture patterns; texture surrounds suppressed the responses to a single line by an average of 42%. Suppression was 7% smaller for lines presented with orientation contrast than for lines presented in a uniform field. Lines at an orientation perpendicular to that of surrounding lines are particularly salient targets that perceptually "pop out" (Treisman, 1985; Treisman & Gormican, 1988; Foster & Ward, 1991; Nothdurft, 1991, 1992). Lines surrounded by similar lines do not pop out. The particular salience of popout targets is largely influenced by the local orientation contrast under which these targets occur (Nothdurft, 1993*b*). The response differences obtained with texture contrast and uniform textures may be a direct reflection of this phenomenon and saliency might simply be the perceptual correlate of the local average activity in V1 (see Nothdurft, 1994*a*,*b*, 1997).

The role of V1 in perceptual popout has been confirmed in evoked potential studies (Bach & Meigen, 1992; Lamme et al., 1992) and in single-cell recordings (Knierim & Van Essen, 1992; Zipser et al., 1996; Kastner et al., 1997). The spatially restricted interaction between the classical RF and nearby surrounds suggests that saliency effects should strongly depend on the texture density, as was confirmed in psychophysical studies (Nothdurft, 1985*b*; Sagi & Julesz, 1987). Also, such interactions are not restricted to differences in texel orientation but have also been found for differences in movement (Nothdurft, 1993; Kastner et al., 1997), spatial frequency (Caelli & Moraglia, 1985; Sagi & Hochstein, 1985; DeAngelis et al., 1994; Li & Li, 1994), and several other properties (Nothdurft, 1993*a*, 1995; Zipser et al., 1996) which all appear to pop out under these circumstances.

The large number of studies which report suppression from optimal stimuli in the surround raises questions about the function of this mechanism. It has been suggested (see Li & Li, 1994, for discussion) that inhibition from beyond the RF could sharpen cells' tuning curves. However, suppression may occur over too large an area to be useful for this particular function. Instead, center-surround interactions of the sort described here may resemble the same sort of center-surround organization found in both retinal and geniculate neurons. The assumed function in those areas is not to sharpen tuning curves but to make cells sensitive to local luminance contrast. Similar interactions among feature detectors in V1 (and in higher areas) may generate sensitivity to feature contrast, which would then allow for the detection of pattern discontinuities. In the normal visual environment such discontinuities are usually associated with the borders of objects.

References

ALBUS, K. & FRIES, W. (1980). Inhibitory sidebands of complex receptive fields in the cat's striate cortex. *Vision Research* **20**, 369–372.

ALLMAN, J., MIEZIN, F. & MCGUINNESS, E.L. (1985). Stimulus specific responses from beyond the classical receptive field: Neurophysiological mechanisms for local-global comparisons in visual neurons. *Annual Review of Neuroscience* **8**, 407–430.

ALLMAN, J., MIEZIN, F. & MCGUINNESS, E.L. (1990). Effects of background motion on the responses of neurons in the first and second cortical visual areas. In *Signal and Sense: Local and Global Order in Perceptual Maps*, ed. EDELMAN, G.M., GALL, W.E. & COWAN, M.W., pp. 131–142. New York: Wiley-Liss.

BACH, M. & MEIGEN, T. (1992). Electrophysiological correlates of texture segregation in the human visual evoked potential. *Vision Research* **32**, 417–424.

BACH, M. & MEIGEN, T. (1997). Similar electrophysiological correlates of texture segregation induced by luminance, orientation, motion and stereo. *Vision Research* **37**, 1409–1414.

BARLOW, H.B., BLAKEMORE, C. & PETTIGREW, J.D. (1967). The neuronal basis of binocular depth discrimination. *Journal of Physiology* (London) **193**, 327–342.

BECK, J. (1967). Perceptual grouping produced by line figures. *Perception and Psychophysics* **2**, 491–495.

BECK, J. (1982). Textural segmentation. In *Organization and Representation in Perception*, ed. BECK, J., pp. 285–317. Hillsdale, New Jersey: Erlbaum.

BISHOP, P.O., COOMBS, J.S. & HENRY, G.H. (1973). Receptive fields of simple cells in the cat striate cortex. *Journal of Physiology* (London) **231**, 31–60.

BLAKEMORE, C. & TOBIN, E.A. (1972). Lateral inhibition between orientation detectors in the cat's visual cortex. *Experimental Brain Research* **15**, 439–440.

BORN, R.T. & TOOTELL, R.B. (1991). Single-unit and 2-deoxyglucose studies of side inhibition in macaque striate cortex. *Proceedings of the National Academy of Sciences of the U.S.A.* **88**, 7071–7075.

CAELLI, T. & MORAGLIA, G. (1985). On the detection of Gabor signals and discrimination of Gabor textures. *Vision Research* **25**, 671–684.

DAS, A. & GILBERT, C.D. (1995). Receptive field expansion in adult visual cortex is linked to dynamic changes in strength of cortical connections. *Journal of Neurophysiology* **74**, 779–792.

DEANGELIS, G.C., FREEMAN, R.D. & OHZAWA, I. (1994). Length and width tuning of neurons in the cat's primary visual cortex. *Journal of Neurophysiology* **71**, 347–374.

DUNCAN, J. & HUMPHREYS, G.W. (1989). Visual search and stimulus similarity. *Psychological Review* **96**, 433–458.

DREHER, B. (1972). Hypercomplex cells in the cat's striate cortex. *Investigative Ophthalmology and Visual Science* **11**, 355–356.

FELLEMAN, D.J. & VAN ESSEN, D.C. (1987). Receptive field properties of neurons in area V3 of macaque monkey extrastriate cortex. *Journal of Neurophysiology* **57**, 889–920.

FELLEMAN, D.J. & VAN ESSEN, D.C. (1991). Distributed hierarchical processing in the primate cerebral cortex. *Cerebral Cortex* **1**, 1–47.

FOSTER, D.H. & WARD, P.A. (1991). Asymmetries in oriented-line detection indicate two orthogonal filters in early vision. *Proceedings of the Royal Society B* (London) **243**, 75–81.

FRIES, W., ALBUS, K. & CREUTZFELDT, O.D. (1977). Effects of interacting visual patterns on single cell responses in cat's striate cortex. *Vision Research* **17**, 1001–1008.

GALLANT, J.L., CONNOR, C.E., RAKSHIT, S., LEWIS, J.W. & VAN ESSEN, D.C. (1996). Neural responses to polar, hyperbolic, and Cartesian gratings in area V4 of the macaque monkey. *Journal of Neurophysiology* **76**, 2718–2739.

GILBERT, C.D. & WIESEL, T.N. (1989). Columnar specificity of intrinsic horizontal and corticocortical connections in cat visual cortex. *Journal of Neuroscience* **9**, 2432–2442.

GILBERT, C.D. & WIESEL, T.N. (1990). The influence of contextual stimuli on the orientation selectivity of cells in primary visual cortex of the cat. *Vision Research* **30**, 1689–1701.

GILBERT, C.D. & WIESEL, T.N. (1992). Receptive field dynamics in adult primary visual cortex. *Nature* **356**, 150–152.

GULYAS, B., ORBAN, G.A., DUYSENS, J. & MAES, H. (1987). The suppressive influence of moving textured backgrounds on responses of cat striate neurons to moving bars. *Journal of Neurophysiology* **57**, 1767–1791.

HAMMOND, P. & SMITH, A.T. (1982). On the sensitivity of complex cells in feline striate cortex to relative motion. *Experimental Brain Research* **47**, 457–460.

HAMMOND, P. & SMITH, A.T. (1984). Sensitivity of complex cells in cat striate cortex to relative motion. *Brain Research* **301**, 287–298.

HENRY, G.H. & BISHOP, P.O. (1971). Simple cells of the striate cortex. In *Contributions to Sensory Physiology, Vol. 5*, ed. NEFF, W.D., pp. 1–46. London, New York: Academic Press.

HUBEL, D.H. & WIESEL, T.N. (1965). Receptive fields and functional architecture in two non-striate visual areas (18 and 19) of the cat. *Journal of Neurophysiology* **41**, 229–289.

HUBEL, D.H. & WIESEL, T.N. (1968). Receptive fields and functional architecture of monkey striate cortex. *Journal of Physiology* (London) **195**, 215–243.

JULESZ, B. (1971). *Foundations of the Cyclopean Perception*. Chicago, Illinois: University Press.

JULESZ, B. (1975). Experiments in the visual perception of texture. *Scientific American* **232**(4), 34–43.

KAPADIA, M.K., ITO, M., GILBERT, C.D. & WESTHEIMER, G. (1995). Improvement in visual sensitivity by changes in local context: Parallel studies in human observers and in V1 of alert monkeys. *Neuron* **15**, 843–856.

KASTNER, S., NOTHDURFT, H.C. & PIGAREV, I.N. (1997). Neuronal correlates of pop-out in cat striate cortex. *Vision Research* **37**, 371–376.

KATO, H., BISHOP, P.O. & ORBAN, G.A. (1978). Hypercomplex and simple/complex cell classifications in cat striate cortex. *Journal of Neurophysiology* **41**, 1071–1095.

KNIERIM, J.J. & VAN ESSEN, D.C. (1992). Neuronal responses to static texture patterns in area V1 of the alert macaque monkey. *Journal of Neurophysiology* **67**, 961–980.

LAMME, V.A.F. (1995). The neurophysiology of figure-ground segregation in primary visual cortex. *Journal of Neuroscience* **15**, 1605–1615.

LAMME, V.A.F., VAN DIJK, B.W. & SPEKREIJSE, H. (1992). Texture segregation is processed by primary visual cortex in man and monkey. Evidence from VEP experiments. *Vision Research* **32**, 797–807.

LAMME, V.A.F., VAN DIJK, B.W. & SPEKREIJSE, H. (1993*a*). Contour from motion processing occurs in primary visual cortex. *Nature* **363**, 541–543.

LAMME, V.A.F., VAN DIJK, B.W. & SPEKREIJSE, H. (1993*b*). Organization of texture segregation processing in primate visual cortex. *Visual Neuroscience* **10**, 781–790.

LAMME, V.A.F., VAN DIJK, B.W. & SPEKREIJSE, H. (1994). Organization of contour from motion processing in primate visual cortex. *Vision Research* **34**, 721–735.

LAMME, V.A.F., ZIPSER, J. & SPEKREIJSE, H. (1997). Figure-ground signals in V1 depend on extrastriate feedback. *Investigative Ophthalmology and Visual Science* **38**, S969.

LI, C.Y. & LI, W. (1994). Extensive integration field beyond the classical receptive field of cat's striate cortical neurons—classification and tuning properties. *Vision Research* **34**, 2337–2355.

MAFFEI, L. & FIORENTINI, A. (1976). The unresponsive regions of visual cortical receptive fields. *Vision Research* **16**, 1131–1139.

MAUNSELL, J.H. & VAN ESSEN, D.C. (1983). The connections of the middle temporal visual area (MT) and their relationship to a cortical hierarchy in the macaque monkey. *Journal of Neuroscience* **3**, 2563–2586.

MCGUIRE, B.A., GILBERT, C.D., RIVLIN, P.K. & WIESEL, T.N. (1991). Targets of horizontal connections in macaque primary visual cortex. *Journal of Comparative Neurology* **305**, 370–392.

MORAGLIA, G. (1989). Display organization and the detection of horizontal line segments. *Perception and Psychophysics* **45**, 265–272.

NAKAYAMA, K. & SILVERMAN, G.H. (1986). Serial and parallel processing of visual feature conjunctions. *Nature* **320**, 264–265.

NELSON, J.I. & FROST, B.J. (1978). Orientation-selective inhibition from beyond the classic visual receptive field. *Brain Research* **139**, 359–365.

NOTHDURFT, H.C. (1985*a*). Orientation sensitivity and texture segmentation in patterns with different line orientation. *Vision Research* **25**, 551–560.

NOTHDURFT, H.C. (1985*b*). Sensitivity for structure gradient in texture discrimination tasks. *Vision Research* **25**, 1957–1968.

NOTHDURFT, H.C. (1990). Texton segregation by associated differences in global and local luminance distribution. *Proceedings of the Royal Society B* (London) **239**, 295–320.

NOTHDURFT, H.C. (1991). Texture segmentation and pop-out from orientation contrast. *Vision Research* **31**, 1073–1078.

NOTHDURFT, H.C. (1992). Feature analysis and the role of similarity in pre-attentive vision. *Perception and Psychophysics* **52**, 355–375.

NOTHDURFT, H.C. (1993*a*). The role of features in preattentive vision: Comparison of orientation, motion, and color cues. *Vision Research* **33**, 1937–1958.

NOTHDURFT, H.C. (1993*b*). The conspicuousness of orientation and motion contrast. *Spatial Vision* **7**, 341–363.

NOTHDURFT, H.C. (1994*a*). Cortical properties of preattentive vision. In *Structural and Functional Organization of the Neocortex*, ed. ALBOWITZ, B., ALBUS, K., KUHNT, U., NOTHDURFT, H.C. & WAHLE, P., pp. 375–384. Heidelberg: Springer.

NOTHDURFT, H.C. (1994*b*). On common properties of visual segmentation. In *Higher-Order Processing in the Visual System*, ed. BOCK, G.R. & GOODE, J.A., pp. 245–268. Chichester: J.A. Wiley (Ciba Foundation Symposium 184).

NOTHDURFT, H.C. (1995). Generalized feature contrast in preattentive vision. *Perception* **24**, 22.

NOTHDURFT, H.C. (1997). Different approaches to the coding of visual segmentation. In *Computational and Biological Mechanisms of Visual Coding*, ed. JENKINS, M. & HARRIS, L., pp. 23–40. New York: Cambridge University Press.

OLAVARRIA, J.F., DEYOE, E.A., KNIERIM, J.J., FOX, J.M. & VAN ESSEN, D.C. (1992). Neural responses to visual texture patterns in middle temporal area of the macaque monkey. *Journal of Neurophysiology* **68**, 164–181.

ORBAN, G.A., KATO, H. & BISHOP, P.O. (1979). Dimensions and properties of end-zone inhibitory areas in receptive fields of hypercomplex cells in cat striate cortex. *Journal of Neurophysiology* **42**, 833–849.

ORBAN, G.A., GULYAS, B. & VOGELS, R. (1987). Influence of a moving texture background on direction selectivity of cat striate cortex neurons. *Journal of Neurophysiology* **57**, 1792–1812.

ROCKLAND, K.S. & LUND, J.S. (1983). Intrinsic laminar lattice connections in primate visual cortex. *Journal of Comparative Neurology* **216**, 303–318.

ROCKLAND, K.S. & VIRGA, A. (1989). Terminal arbors of individual "feedback" axons projecting from area V2 to V1 in the macaque monkey: A study using immunohistochemistry of anterogradely transported Phaseolus vulgaris-leucoagglutinin. *Journal of Comparative Neurology* **285**, 54–72.

SAGI, D. (1995). The psychophysics of texture segmentation. In *Early Vision and Beyond*, ed. PAPATHOMAS, P.V., CHUBB, C., GOREA, A. & KOWLER, E., pp. 69–78. Cambridge, Massachusetts: MIT Press.

SAGI, D. & HOCHSTEIN, S. (1985). Lateral inhibition between spatially adjacent spatial-frequency channels? *Perception and Psychophysics* **37**, 315–322.

SAGI, D. & JULESZ, B. (1987). Short-range limitations on detection of feature differences. *Spatial Vision* **2**, 39–49.

SILLITO, A.M., CUDEIRO, J. & MURPHY, P.C. (1993). Orientation sensitive elements in the corticofugal influence on centre-surround interactions in the dorsal lateral geniculate nucleus. *Experimental Brain Research* **93**, 6–16.

SILLITO, A.M., GRIEVE, K.L., JONES, H.E., CUDEIRO, J. & DAVIS, J. (1995). Visual cortical mechanisms detecting focal orientation discontinuities. *Nature* **378**, 492–496.

TREISMAN, A. (1985). Preattentive processing in vision. *Computer Vision, Graphics, and Image Processing* **31**, 156–177.

TREISMAN, A. & GORMICAN, S. (1988). Feature analysis in early vision: Evidence from search asymmetries. *Psychological Review* **95**, 15–48.

TS'O, D.Y. & GILBERT, C.D. (1988). The organization of chromatic and spatial interactions in the primate striate cortex. *Journal of Neuroscience* **8**, 1712–1727.

TS'O, D.Y., GILBERT, C.D. & WIESEL, T.N. (1986). Relationships between horizontal interactions and functional architecture in cat striate cortex as revealed by cross-correlation analysis. *Journal of Neuroscience* **6**, 1160–1170.

ZIPSER, K., LAMME, V.A.F. & SCHILLER, P.H. (1996). Contextual modulation in primary visual cortex. *Journal of Neuroscience* **16**, 7376–7389.

ZIPSER, J., LAMME, V.A.F. & SPEKREIJSE, H. (1997). Figure/ground signals in V1 eliminated by anesthesia. *Investigative Ophthalmology and Visual Science* **38**, S969.